

RESEARCH ARTICLE

Improved Brain Tumor Segmentation and Classification in Brain MRI With FCM-SVM: A Diagnostic Approach

SAMAR M. ALQHTANI¹, TOUFIQUE AHMED SOOMRO², (Senior Member, IEEE), AHMED ALI SHAH³, (Senior Member, IEEE), ABDUL AZIZ MEMON⁵, (Member, IEEE), MUHAMMAD IRFAN⁴, SAIFUR RAHMAN⁴, MOHAMMED JALALAH⁴, ABDULKAREM H. M. ALMAWGANI⁴, AND LADON AHMED BADE ELJAK⁵

¹Department of Information Systems, College of Computer Science and Information Systems, Najran University, Najran 61441, Saudi Arabia

²Department of Electronics Engineering, The University of Larkano, Larkana, Sindh 75660, Pakistan

³Department of Electrical Engineering, Sukkur IBA University, Sukkur 65200, Pakistan

⁴Department of Electrical Engineering, College of Engineering, Najran University, Najran 61441, Saudi Arabia

⁵Department of Electrical and Electronic Engineering, Sudan Technological University, Khartoum 11115, Sudan

Corresponding author: Ladon Ahmed Bade Eljak (ladon.ahmed@gmail.com)

This work was supported by the Deanship of Scientific Research, Najran University, Kingdom of Saudi Arabia, under the Distinguish Research funding program Grant code Number (NU/DRP/SERC/12/7).

ABSTRACT Cancer associated with the nervous system and brain tumors ranks among the leading causes of death in various countries. Magnetic resonance imaging (MRI) and computed tomography (CT) capture brain images. MRI is pivotal in diagnosing brain tumors and analyzing other brain disorders. Typically, radiologists or experts manually assess MRI images to detect brain tumors and abnormalities in the early stages for appropriate treatment. However, early brain tumor diagnosis is complex, necessitating computerized methods. This research introduces a novel approach for the automated segmentation of brain tumors and a framework for classifying brain tumor regions. The proposed methods comprise several stages: preprocessing, enhancing the coherence of MRI brain images using Contrast Limited Adaptive Histogram Equalization (CLAHE) and diffusion filtering in the first two steps, followed by the segmentation of the region of interest using the Fuzzy C-Means (FCM) clustering technique in the third step. The last step involves classification using the Support Vector Machine (SVM) classifier. The classifier is applied to different brain tumor types, from meningioma to pituitary tumors, utilizing the CE-MRI database. The proposed method exhibits significantly improved contrast and proves the effectiveness of the classification framework, achieving an average sensitivity of 0.977, specificity of 0.979, accuracy of 0.982, and a Dice score (DSC) of 0.961. Furthermore, this method demonstrates a shorter processing time of 0.42 seconds compared to existing approaches. The performance of this method underscores its significance when compared to state-of-the-art methods in terms of sensitivity, specificity, accuracy, and DSC. For future enhancements, it is possible to standardize the approach by incorporating a set of classifiers to increase the robustness of the brain classification method.

INDEX TERMS Brain tumor, segmentation, classification, diffusion filtering, contrast limited adaptive histogram equalization, Fuzzy C-Means, support vector machine.

I. INTRODUCTION

In e-health, medical experts strive to enhance patients' healthcare efficiency by adopting digital medical technology.

The associate editor coordinating the review of this manuscript and approving it for publication was Sudhakar Radhakrishnan¹.

Within this context, the field faces intricate challenges, particularly in the domain of magnetic resonance imaging (MRI) of the brain. The brain, a remarkably intricate component of the human body, orchestrates the operation of billions of cells [1]. Brain tumors, constituting an unregulated proliferation of abnormal cells within the brain, profoundly disrupt the brain's

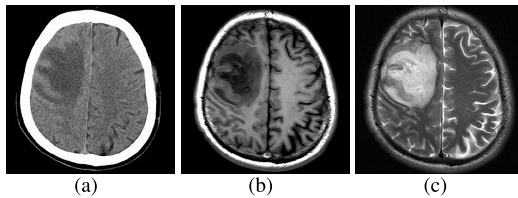


FIGURE 1. The comparison of CT images and MRI images of the brain. The brain CT images (Fig A) showed the hypodensity of the right frontal lobe of the brain and the T1 and T2 weighted MRI images (Fig B and C) also showed the hypointensity of the lesion with less noise and gives better image representation.

normal functioning [2]. This abnormal cell growth exerts a substantial toll on the patient's well-being [3]. To address this critical issue, computerized techniques emerge as a viable solution for the early detection of brain tumors. These techniques excel in isolating abnormal regions within brain MRI scans, primarily relying on image segmentation and classification methodologies. The components of the brain, including gray matter, white matter, and cerebrospinal fluid, are intricately involved in this process, and image segmentation techniques prove invaluable for their precise extraction [4], [5]. Researchers commonly leverage brain MRI images to identify and expedite the treatment of brain abnormalities. The quality of these MRI images significantly impacts the depth of insight into brain structure and associated cell anomalies, underscoring the importance of acquiring high-quality images [6], [7].

While several methods are available for capturing brain images, MRI is a more resilient and efficient choice compared to computed tomography (CT). CT scans of the brain may exhibit superior contrast; however, they often suffer from noise, restricting the radiologist's ability to evaluate medical images thoroughly. Figure 1 offers a visual comparison between CT and MRI brain images [8], [9]. Notably, the brain CT images reveal hypodensity in the right frontal lobe. In contrast, the T1 and T2 weighted MRI scans also depict lesion hypointensity but with reduced noise, providing a superior image representation. Brain tumors exhibit diverse classifications based on their behavior and therapeutic considerations, and the optimal management of these tumors helps minimize the necessity for biopsies by effectively categorizing them into benign and malignant types.

Various techniques are employed to identify brain tumors within brain MRI images. Primarily, clustering techniques, such as color-based and histogram methods, are applied to enhance the precision of tumor detection. Subsequently, classifiers come into play to distinguish between normal and abnormal tumor regions, with neural network-based classifiers predominantly serving this purpose [10], [11], [26]. Nevertheless, these segmentation and classification methodologies exhibit several limitations, including a decline in accuracy, noise, variations in contrast, intensity irregularities, computational complexity, intricacies in feature

selection, and time-consuming processes [12], [13]. We have proposed a novel approach focusing on image denoising and improving overall detection performance to address these challenges and enhance tumor detection accuracy.

In essence, the distinctiveness of the article is rooted in its introduction of an innovative framework for the automated segmentation and classification of brain tumors within brain MRI images. This research work introduces a novel framework for automated brain tumor diagnosis through MRI analysis, offering distinct advancements over existing methods. The proposed automated segmentation pipeline, starting with innovative preprocessing techniques like contrast-limited adaptive histogram equalization (CLAHE) and diffusion filtering, streamlines identifying and classifying brain tumors within MRI images. Using the Fuzzy C-Means (FCM) algorithm for segmentation and integrating a Support Vector Machine (SVM) classifier for categorizing brain tumor regions represent significant methodological improvements. Evaluating a Contrast-Enhanced Magnetic Resonance Imaging (CE-MRI) database encompassing diverse brain tumor types validates the method's efficacy and facilitates comparisons with alternative classifiers. The proposed framework exhibits enhanced performance metrics, including superior sensitivity, specificity, accuracy, and Dice Score (DSC), highlighting its proficiency in precise tumor identification. Moreover, the method's remarkable time-efficient processing, with a duration of only 0.42 seconds, surpasses conventional approaches, showcasing its potential for practical implementation in clinical settings. Overall, the article's distinct contributions lie in its innovative pipeline, advanced algorithms, and superior performance metrics, positioning it as a noteworthy advancement in automated brain tumor diagnosis compared to existing methods. Here, we enumerate the key contributions that underscore its novelty:

- **Automated Segmentation Pipeline:** This research introduces an automated pipeline, encompassing multiple sequential stages, to streamline the segmentation and classification of brain tumors within MRI images. It commences with preprocessing steps, employing techniques like contrast-limited adaptive histogram equalization (CLAHE) and diffusion filtering to enhance and coalesce MRI brain images in preparation for subsequent segmentation and classification.
- **FCM Based Segmentation:** Within this proposed pipeline, the FCM algorithm takes center stage for segmenting abnormal regions in brain images. FCM is recognized for its efficacy in delineating structures in medical images.
- **SVM Based Classification:** The pipeline leverages a Support Vector Machine classifier to categorize brain tumor regions. SVMs are widely acclaimed in machine learning for their capacity to tackle intricate classification tasks.
- **Evaluation using CE-MRI Database:** The effectiveness of this pipeline is thoroughly assessed using a

Contrast-Enhanced Magnetic Resonance Imaging (CE-MRI) database with image 512×512 , encompassing a diverse array of brain tumors, including meningioma and pituitary tumors. This evaluation substantiates its efficacy across various tumor types and facilitates comparisons with alternative classifiers and methods.

- **Enhanced Performance:** The results generated by this proposed pipeline manifest superior contrast and efficiency when contrasted with existing methodologies. It attains remarkable average sensitivity, specificity, accuracy, and Dice Score (DSC), affirming its proficiency in precisely identifying and classifying brain tumor regions.
- **Time-Efficient Processing:** Significantly, the proposed method exhibits a shorter processing time of merely 0.42 seconds in contrast to conventional approaches. This attribute holds substantial importance for practical implementation in clinical settings, where prompt diagnosis remains a pivotal consideration.

The primary aim of this research endeavor revolves around the segmentation of brain tumors and the subsequent classification of their stage based on brain MRI images. The analysis of these images presents a formidable challenge due to the multifaceted processing issues inherent in computerized brain MRI images. To tackle this challenge, the proposed methodology comprises five distinctive stages. In the initial stage, brain MRI images undergo preprocessing, which includes noise elimination. The second stage centers on harmonizing the brain MRI images, a crucial step since these images often exhibit non-coherent regions, complicating ensuring consistency in the contrast between foreground and background elements. The third stage focuses on contrast adjustment due to the persistent presence of varying contrast regions. The fourth stage is dedicated to segmenting abnormal or tumor regions within the images, while the final stage encompasses the classification of the identified brain tumors. Importantly, all these stages are underpinned by innovative image-processing techniques.

II. RELATED WORK

The incidence of brain tumors has seen a significant increase, ranging from 10% to 15% between 2004 and 2020, underscoring the pressing need to address this health crisis. In the field of medical diagnostics, advanced imaging technologies, such as computed tomography (CT) and magnetic resonance imaging (MRI), have become indispensable for detecting and understanding central nervous system (CNS) disorders [14]. MRI, in particular, stands out as a noninvasive diagnostic tool, providing detailed cross-sectional images of the brain that enable healthcare professionals to examine brain anatomy intricacies with exceptional sensitivity [15]. Despite the promise of these imaging techniques, their effective use relies on the expertise of medical specialists, and interpreting the wealth of information they convey remains a meticulous and time-intensive process [16]. Enhancing healthcare

providers' skills in this domain is imperative for accurately diagnosing CNS disorders [17]. Magnetic resonance imaging (MRI) has emerged as the foremost technique for detecting and classifying brain tumors (BTs), encompassing distinct modalities such as T1-weighted MRI (T1), T2-weighted MRI (T2), T1-weighted contrast-enhanced MRI (T1-CE), and fluid-attenuated inversion recovery (FLAIR) [18], [19], [20]. Utilizing software-based tools alongside MRI scans facilitates the segmentation, identification, and categorization of tumors, expediting treatment strategies and contributing to improved patient survival rates [18], [21], [22], [23]. Consequently, software specialists are increasingly focused on developing tumor detection systems, particularly emphasizing image processing techniques [Isn2016]. The growing volume of image datasets, fueled by the widespread adoption of digital cameras and imaging technologies, poses a challenge, making it essential to address the management and analysis of these extensive datasets [25].

The segmentation and precise classification of brain tumor regions, utilizing a combination of machine learning and image processing, pose a formidable challenge, given the multitude of methodologies proposed for brain tumor detection within brain MRI images [27]. The related work section discusses various recently introduced methods addressing this issue. One recent study introduced a computerized approach to brain tumor classification. This method hinged on the Harmony Search Algorithm (HCS) optimization technique to train a multi-class Support Vector Neural Network (SVNN) [39]. The approach incorporated the Bayesian fuzzy clustering method to identify tumors in MRI images automatically. For this purpose, an array was constructed using the HCS optimization technique, which involved the deployment of multiple multi-class Support Vector Neural Networks (multi-SVNNs). Notably, the study exclusively centered on the BRATS dataset, and its findings may not be broadly applicable to other datasets. Several similar techniques have also been proposed that use brain MRI images for brain tumor detection, employing the Bayesian fuzzy clustering method in conjunction with the HCS optimization algorithm [28], [29]. Notably, these HCS optimization algorithms have outperformed existing methods in certain contexts [30]. However, it's important to note that implementing these techniques is typically restricted to a limited set of images from the Brain Tumor Segmentation (BraTS) database and may not be directly transferable to other databases [27].

Yin et al. [31] introduced a method structured around three key steps: background correction, the segmentation of abnormal regions, and the classification of brain tumors. Their approach incorporated a multilayered perception neural system and utilized whale optimization algorithms rooted in disarray hypothesis and procedural base mapping to attain optimal brain tumor segmentation and classification results. However, it's important to note that this algorithm did not yield a notable enhancement in accuracy. In a distinct study, Alagarsamy et al. [32] presented an enhanced brain image

segmentation technique called BAT-IT2FCM (Bat Algorithm and Interval Type-2 Fuzzy C-Means clustering). This method draws upon BAT calculations to discern the most suitable groupings within the IT2FCM clustering process. Although this approach improved accuracy, it relies on threshold factors and necessitates a more extended processing time.

Kumar et al. [33] introduced the Weighted Correlation Feature Selection-Based Iterative Bayesian Multivariate Deep Neural Learning (WCFS-IBMDNL) method for early-stage brain tumor analysis. It employed an Iterative Bayesian Multivariate Deep Neural Network (WC-FS) to select pertinent medical features that formed the model for brain tumor regions. However, their use of the Iterative Bayesian Multivariate Deep Neural Network (IBMDNN) classifier led to false pixel detection, ultimately diminishing method accuracy. Ozyurt et al. [34] implemented a hybrid approach, combining Neutrosophy with Convolutional Neural Network (NS-CNN) for tumor region characterization in brain images. They utilized brain MRI images segmented using the neuromorphic ensemble main, employing the extreme fuzzy sure entropy method. While their approach, which harnessed three classifiers (CNN, Support Vector Machine, and K-Nearest Neighbors), demonstrated enhanced accuracy, the neurotrophic method's inconsistency in the CNN structure adversely affected overall performance.

Selvapandian and Manivannan [35] employed the non-subsampled contourlet transform (NSCT) to enhance brain images and extract tumors. They utilized the Adaptive Neuro Fuzzy Inference System (ANFIS) to distinguish between typical and glioma brain images. Tumor regions within glioma brain images were extracted using morphological operations, but the proposed method yielded only satisfactory results on BRATS. Sharif et al. [36] proposed a brain image analysis method that involved the removal of the cranial part of brain images using brain surface extraction (BSE) techniques. This process eliminated the skull based on images using particle swarm optimization (PSO) for improved image segmentation. Subsequently, the local binary model technique was employed to extract brain tumor regions, with an Artificial Neural Network (ANN) classifier for tumor classification. However, limitations in optimizing the tumor substructure location impacted method accuracy.

Sharma et al. [37] introduced a hybrid approach combining the k-means algorithm with Artificial Neural Networks (ANN) for brain tumor detection. They employed the Gray-Level Co-Occurrence Matrix (GLCM) for feature extraction and utilized a fuzzy inference system for classification, with tumor segmentation accomplished using the K-means algorithm. While their method demonstrated enhanced performance, it occasionally flagged false pixels, particularly in the case of smaller tumors. In a separate study, Shree et al. [38] based their brain tumor detection and classification on Discrete Wavelet Transformation (DWT) and Probabilistic Neural Networks (PNN). Features were extracted using GLCM, and the brain tumor region was segmented using

DWT. This approach not only improved performance but also streamlined the complexity of tumor segmentation. The PNN was trained and tested on brain MRI images, yielding satisfactory results.

A two-phase multidimensional approach was employed in a study to distinguish between brain tumors and healthy brain tissue. In the first phase, Convolutional Neural Networks (CNNs) were utilized for preprocessing and feature selection, while the second phase focused on classification using Error-Correcting Output Codes Support Vector Machines (ECCOSVM). To attain the highest accuracy, which reached 99.55%, the first phase employed Visual Geometry Group-19 (VGG-19), Visual Geometry Group-16 (VGG-16), and AlexNet, with AlexNet proving to be the most successful. The study drew data from the BraTS and RIDER databases [40]. In another study, SVM and Otsu thresholding were used for brain tumor classification [41]. However, a comparative analysis revealed that the method's accuracy required improvement. To address this issue, Molina-Torres employed a kernel SVM approach utilizing the Gaussian Radial Basis (GRB) kernel for brain tumor classification and assessed performance using metrics like specificity, precision, and accuracy [42].

Numerous investigations have explored brain tumor detection using diverse methodologies and deep learning models [27]. However, some studies lack performance comparisons between proposed models and traditional machine-learning approaches, and specific models have been criticized for their computationally intensive processes [27], [43]. Additionally, many relevant studies focus on classifying three types of brain tumors, often neglecting data related to healthy subjects [44]. From a scientific standpoint, diagnosing tumors through medical imaging is prone to errors and heavily depends on radiologists' expertise. Given the variability in pathology and the potential for human specialists to experience fatigue, a compelling argument exists for integrating computer-assisted interventions in medical imaging [27]. Computational intelligence-oriented techniques, particularly deep learning ones, play a crucial role in analyzing, segmenting, and classifying cancer images, specifically on brain tumors [45]. These approaches offer a promising avenue to assist researchers and physicians in identifying and categorizing brain tumors. Despite the substantial efforts invested in brain tumor detection research, several limitations persist, underscoring the need for a novel algorithm that leverages MR images to enhance the accuracy and reliability of brain tumor detection—notably, existing research work, particularly in preprocessing, warrants improvement for enhanced performance. In the following section, we delve into the methodology of the proposed approach.

III. PROPOSED METHOD

Brain MRI images are preferred in medical imaging due to the non-invasive nature of MRI, which eliminates the risk

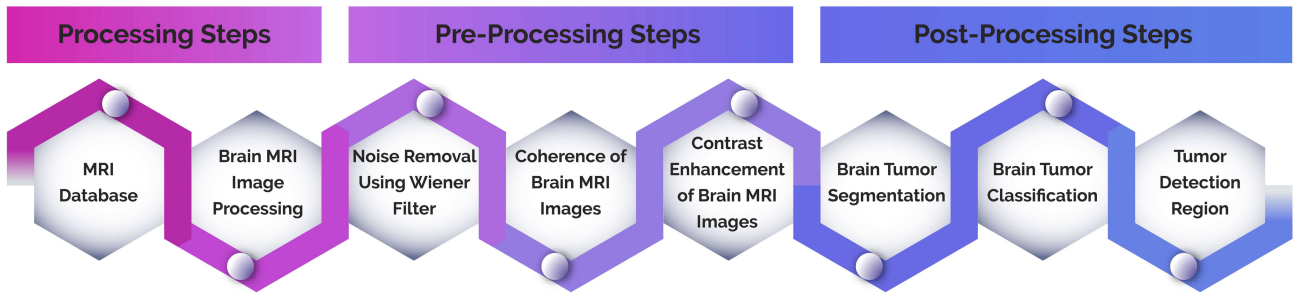


FIGURE 2. The Proposed Method steps for segmentation and classification of Brain MRI Images.

of radiation exposure, making it safe for the human body. Moreover, MRI scans offer a multi-dimensional analysis that surpasses other imaging modalities like computed tomography and X-ray images. While brain MRI image segmentation is primarily employed for brain tumor delineation, manual segmentation is time-consuming and can be challenging to achieve with pinpoint accuracy. In this research paper, we introduce a novel approach featuring five distinct steps for the computerized classification and segmentation of brain MRI images in the context of brain tumor detection.

The primary objective of this method is to identify tumor areas within brain MRI images. Illustrated in Figure 2, this proposed approach is a computer-based solution designed to detect abnormal brain MRI findings. It relies on coherent contrast, coupled with classification and segmentation tasks for brain tumor detection. The method unfolds in four sequential steps, with the first two comprising the preprocessing stage. The initial step focuses on image processing for brain MRI images, aiming to address inconsistencies in the MRI data. To rectify these inconsistencies, the second step delves into enhancing the coherence of brain MRI images through oriented diffusion filtering. The subsequent two steps form the post-processing stage. The third step involves binary segmentation of brain tumors using the FCM method, while the fourth step employs a support vector machine classifier for brain tumor classification. This cohesive algorithm is recognized as a computerized solution for detecting brain tumors within brain MRI images.

A. BRAIN MRI IMAGE PROCESSING

The processing of brain MRI images constitutes a crucial step within the pre-processing stage of the proposed method. Brain MRI image processing primarily revolves around data enhancement and the reduction of noise levels. In this study, we performed image processing on brain MRI scans acquired from three different planes, specifically the axial, sagittal, and coronal planes, all sourced from the CE-MRI database.

A 5 by 5 Wiener filter was employed to alleviate noise in brain MRI images, as depicted in Figure 3. The Wiener filter is a mathematical technique specifically designed for noise reduction in brain MRI images. It hinges on two key parameters: the local window for each pixel, which, in this

instance, utilized the 5 by 5 Wiener filter, and the noise variance.

The Wiener filter operates on a local window encompassing each pixel, and the output at each pixel is computed using Equation 1. This equation encompasses the Wiener filter, the local mean of the input image, and convolution. Subsequently, the Wiener filter is determined using Equation 2 and 3, which considers the local variance of the input image within the pixel's vicinity and the variance associated with the noise. The mathematical steps involved in the Wiener filtering process can be enumerated as follows:

- 1) The Mean of noise contained image is calculated accordingly to provide the mask. Equation 1 is a representation of the mathematical problem for this step

$$\mu = \frac{1}{NM} \sum_{n_1=1}^N \sum_{n_2=1}^M I(n_1, n_2). \quad (1)$$

The $N - by - M$ local neighborhood of each pixel in the image is used for this calculation.

- 2) The Variance of the noisy image is calculated accordingly to provide the mask. Equation 2 is a representation of the mathematical problem for this step.

$$\mu = \frac{1}{NM} \sum_{n_1=1}^N \sum_{n_2=1}^M I^2(n_1, n_2) - \mu^2. \quad (2)$$

The $N - by - M$ local neighborhood of each pixel in the image is used for this calculation.

- 3) Utilising these estimates, a pixel-wise Wiener filter is created by the adaptive Wiener. Equation 3 is a representation of the mathematical problem in this step.

$$F(n_1, n_2) = \mu + \frac{\sigma^2 + v}{\sigma^2} (I(n_1, n_2) - \mu). \quad (3)$$

Accordingly, the noise variance is v . However, when no noise variance is given, then adaptive Wiener filter will take an average of all of the estimated local variances for use.

Once the noise reduction is accomplished in the proposed method's first step, attention is turned to addressing the

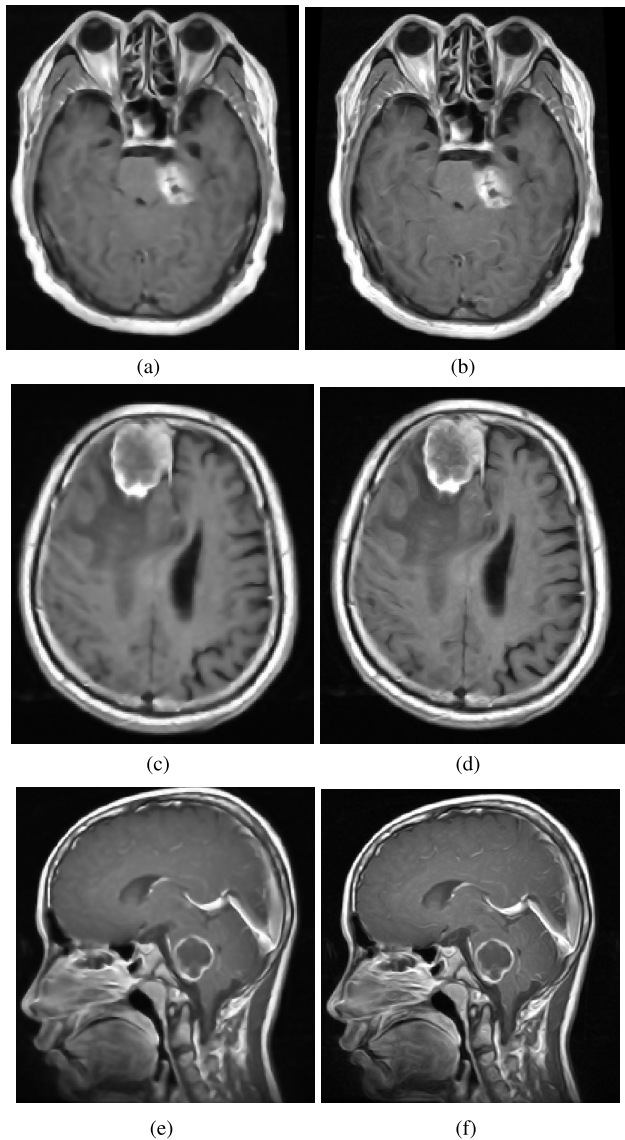


FIGURE 3. Enhanced the clarity of brain MRI: comparison of original and filtered images on the axial, sagittal and coronal planes. The first row shows the original and filtered images in the axial planes. The second row shows original and filtered images in the sagittal planes. The third row shows original and filtered images in the coronal planes.

issue of variable low-contrast regions observed in brain MRI images in the subsequent step as shown in Figure 3.

B. COHERENCE OF BRAIN MRI IMAGES

Following the noise reduction process, non-coherent regions remain challenging within brain MRI images, making it intricate to identify tumor-affected areas. These non-coherent regions often appear in multiple sections within a single image. To overcome this challenge, oriented diffusion filtering is the initial step in brain MRI tumor detection.

Oriented diffusion filtering necessitates calculated orientation data derived from regions within the image, known as the orientation (OF) field. This information guides the diffusion tensor to align with the appropriate direction of detail

consistency within the image [46]. Achieving coherence within the MRI image of the brain is imperative, as it enables better visualization of details crucial for brain tumor detection. For this purpose, we adopted the optimization scheme of the Anisotropic Diffusion Filter [47]. This process encompasses the following steps:

- 1) Computation of the second-moment matrix for each pixel within the brain MRI region.
- 2) It ensures that each pixel within the region possesses its unique diffusion matrix.
- 3) Compute the intensity change for each pixel within the region, given by $\nabla(D\nabla L)$.
- 4) Image refinement using the difference formula defined in equation 4. This leads to a coherent image, as illustrated in Figure 4.

$$f^{t+\Delta t} = f^t + \Delta t \times \nabla(D\nabla f). \quad (4)$$

The utilization of oriented diffusion filtering aids in addressing the challenge of non-coherence within brain MRI images, thereby improving the accuracy of tumor detection.

A comprehensive image analysis of the coherent process has been conducted, as illustrated in Figure 5. It is evident from the analysis that the brain tumor region, indicated by the yellow circle, is more perceptible and coherent in the processed image. Furthermore, the matter anatomy, denoted by the red rectangle, is distinctly analyzed with uniform contrast in the coherent image. However, it is important to note that this output can potentially lead to an improper segmentation of the brain tumor region.

C. CONTRAST ENHANCEMENT OF BRAIN MRI IMAGES

Contrast-limited adaptive histogram equalization (CLAHE) is employed to prevent excessive contrast amplification, a crucial consideration when dealing with small brain tumor regions in MRI images. The rationale behind choosing CLAHE lies in its operation at the tile level, aligning with the localized nature of brain tumor regions in MRI images. The process can be deconstructed into several key steps to comprehend the mathematical underpinnings of CLAHE in the context of brain MRI images. Firstly, the image is divided into smaller regions or tiles. Next, the pixel intensity histogram is computed for each tile. A contrast limiting function is applied to reduce the number of pixels with extreme values. Subsequently, the histogram within each tile is redistributed through histogram equalization. Finally, the processed tiles are combined to reconstruct the original image. The contrast limiting function embedded within CLAHE is mathematically defined by Equation 5, where k serves as a constant governing the extent of contrast limitation, L signifies the minimum pixel intensity value within the tile, and L_{\max} denotes the maximum pixel intensity value within the tile.

$$f(x) = \begin{cases} 0, & \text{if } x < L \\ k(x - L), & \text{if } L \leq x \leq L_{\max} \\ k(L_{\max} - L), & \text{if } x > L_{\max} \end{cases} \quad (5)$$

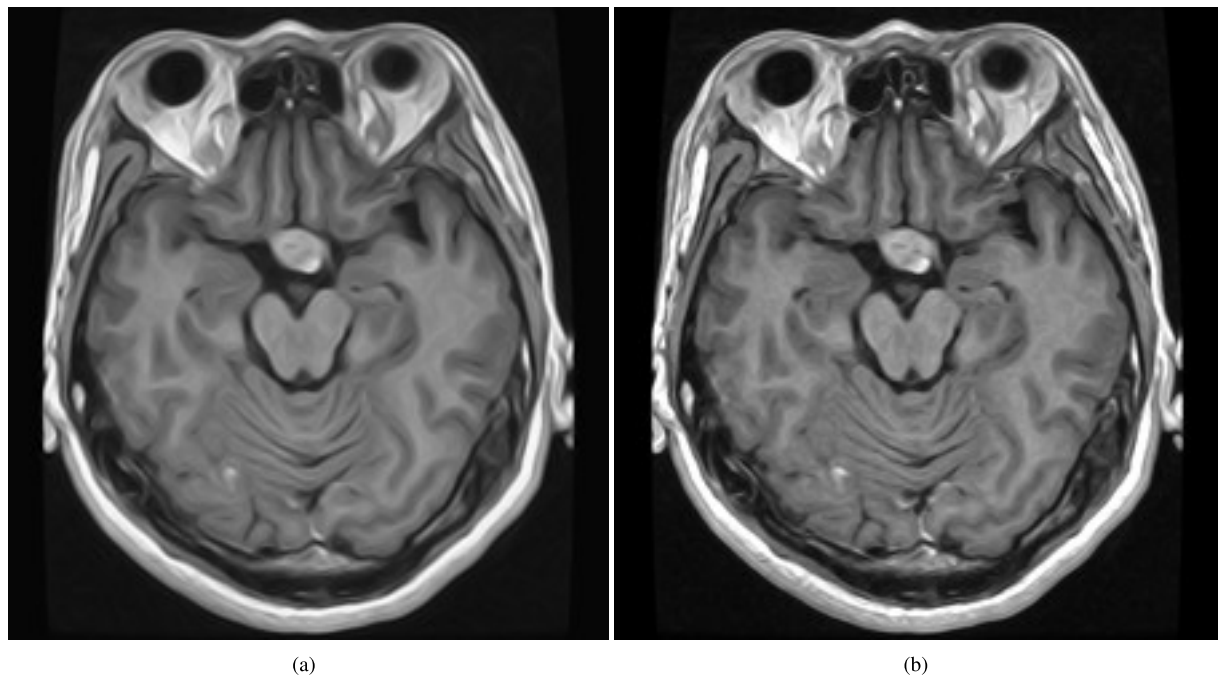


FIGURE 4. Improving Clarity in Brain MRI Images: Transitioning from Non-Coherent (Fig(a)) to Coherent (Fig(b)). It is evident that non-coherent images lack clarity, especially in terms of matter anatomy, which significantly affects the tumor region. On the other hand, the coherent image in Fig(b) illustrates enhanced matter anatomy with uniformity. Further enhancement provides a more detailed analysis.

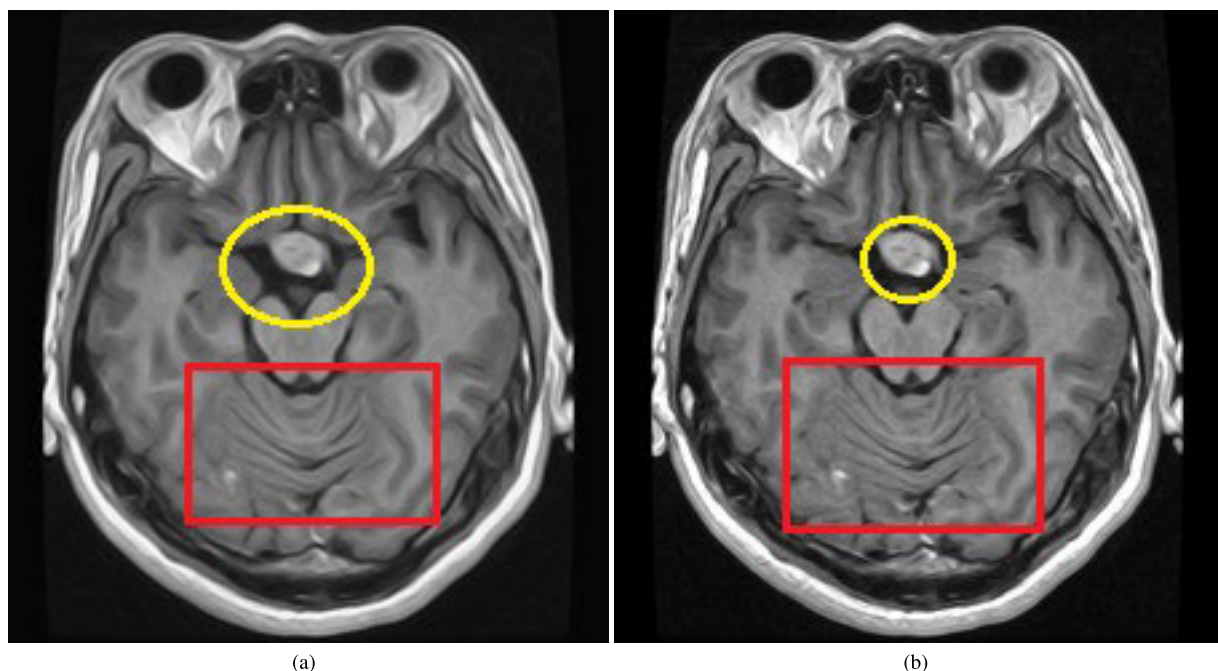


FIGURE 5. Detailed analysis of the coherent process. The yellow circle highlights the enhanced visibility of the brain tumor region, while the red rectangle indicates a clear analysis of matter anatomy with uniform contrast in the coherent image. Note that this output may result in improper segmentation of the brain tumor region.

Histogram equalization, on the other hand, is a technique employed to enhance image contrast by redistributing pixel intensities. This is achieved by calculating the image's cumulative distribution function (CDF) and then mapping

each pixel intensity to a new value based on the CDF. Consequently, the image exhibits a more uniform distribution of pixel intensities, thus bolstering its contrast. CLAHE uniquely performs histogram equalization within each image

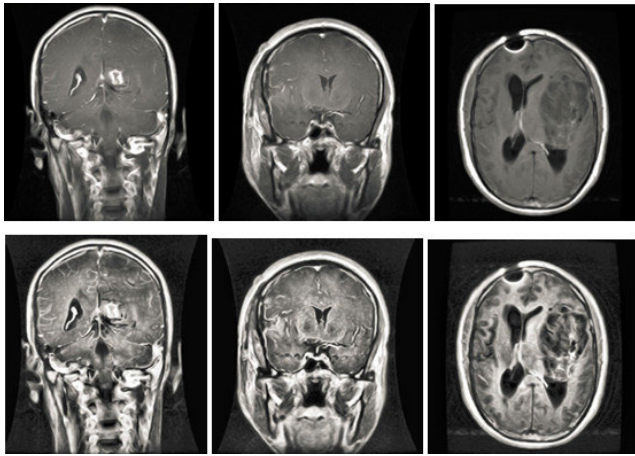


FIGURE 6. The enhanced image from CLAHE reveals a more prominent depiction of the brain tumor area. The first row displays the coherent image, while the second row showcases the CLAHE output image.

tile rather than applying it globally to the entire image. This localized approach helps prevent the amplification of noise or artifacts that may be present in the image while preserving the local contrast details. Consequently, CLAHE produces a more detailed image with improved contrast. CLAHE plays a pivotal role in enhancing the contrast of medical images, including Magnetic Resonance Imaging (MRI) in this research, as it reveals critical features and structures within brain MRI images that might be challenging to discern otherwise. The output of CLAHE is depicted in Figure 6, illustrating its impact on enhancing image contrast.

D. POST-PROCESSING: SEGMENTATION OF BRAIN TUMOR REGION BASED ON FCM

Fuzzy C-means (FCM) segmentation is vital in extracting brain tumor regions from MRI images. This technique is instrumental in creating an initial binary representation of the brain MRI images, serving as a foundation for further analysis and classification. FCM assigns pixels to multiple classes, each with a membership function level between 0 and 1. The goal of FCM is to determine the cluster centers that best represent the pixel distribution within the image. Mathematically, the FCM model can be expressed as follows:

Given a set of brain MRI images, let X represent the image domain. Each pixel x_i within this domain is assigned a membership function u_{ij} , where j denotes the class index. The FCM algorithm aims to find c_j cluster centers that best characterize the pixel distribution for the given set of images. The goal is to minimize the following objective function:

$$J(U, C) = \sum_{i=1}^N \sum_{j=1}^M u_{ij}^m \|x_i - c_j\|^2. \quad (6)$$

In this equation 6, $J(U, C)$ represents the objective function to be minimized. N is the total number of pixels in the image. M is the number of classes (clusters). u_{ij} is the

membership value for pixel x_i in class j . m is the fuzziness exponent (typically set to 2 for FCM). x_i is the pixel in the image. c_j is the cluster center for class j . The FCM algorithm operates iteratively to optimize the cluster centers c_j and the membership values u_{ij} . The steps involved in FCM are as follows:

- 1) Initialization: Start with an initial estimate of cluster centers c_j .
- 2) Membership Calculation: Compute the membership values u_{ij} for each pixel x_i indicating the likelihood of belonging to each class.
- 3) Update Cluster Centers: Recalculate the cluster centers c_j using the updated membership values.
- 4) Convergence Check: Determine if the algorithm has reached convergence. If not, repeat steps 2 and 3.
- 5) Termination: Once convergence is achieved, the algorithm concludes, providing the cluster centers c_j and the membership values u_{ij} .

In the context of brain MRI images, FCM is employed to identify the actual pixels belonging to the tumor region. This pre-processing step is pivotal in improving the accuracy of subsequent classification methods, such as Support Vector Machine (SVM). By accurately delineating the tumor region through FCM, SVM can then effectively classify it. The FCM model essentially seeks to find the best cluster centers that represent the pixel distribution within the brain MRI images, with the goal of accurately segmenting the tumor regions. In our approach, the SVM classifier as it is last step of proposed method as elaborated in section III-E receives the segmented output generated by the Fuzzy C-Means (FCM) algorithm as its input. Specifically, the SVM classifier operates on features extracted from the segmented regions, particularly from the cluster 2 output image. Both the FCM cluster 1 output and cluster 2 output are depicted in the Figure as segmented images. The segmented images serve as the SVM classifier's input, contributing to the accurate detection of the brain tumor region.

E. BRAIN TUMOR CLASSIFICATION

The final step of our proposed method is classification of brain tumor by using Support Vector Machine (SVM). SVM is the supervised learning method based on statistical learning theory to classify data [50]. The first step, data labeling is necessary for the training dataset to be represented as $D = \{|x, y| | x \rightarrow \text{datasample}, y \rightarrow \text{claslabel}\}$. The main task of SVM is to calculate functions that represent with f such as $f(x) = y$ for all image data or image pixels with the aim of classifying the brain tumor. Hinge loss function is a mathematical function commonly used SVM for binary classification tasks, including those involving brain MRI images. It quantifies the "loss" or "cost" associated with misclassifying data points and encourages the SVM to find a decision boundary (hyperplane) that separates the two classes with a certain margin. Mathematically, the hinge loss $L(y,$

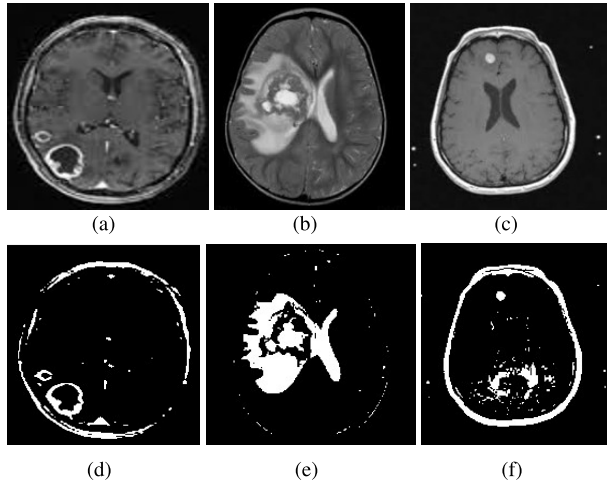


FIGURE 7. Segmentation results from the Fuzzy C-Means (FCM) algorithm are depicted, with Row 01 illustrating the cluster 1 output and Row 02 representing the cluster 2 output. The segmented 2 image, serving as the input to the Support Vector Machine (SVM) classifier, plays a pivotal role in achieving the accurate detection of the brain tumor region.

$f(x)$ for a single data point (x, y) is defined as:

$$L(y, f(x)) = \max(0, 1 - y * f(x)). \quad (7)$$

where:

- y is the true class label of the data point (-1 or 1, for binary classification).
- $f(x)$ is the SVM's decision function output for that data point. It represents the signed distance of the data point to the decision hyperplane.

The hinge loss has the following characteristics:

- 1) When the data point is correctly classified ($y * f(x) > 1$), the loss is 0, indicating no penalty for correct classifications.
- 2) When the data point is misclassified and lies on the correct side of the decision margin ($0 < y * f(x) < 1$), the loss increases linearly as the distance from the margin decreases.
- 3) When the data point is misclassified and lies on the wrong side of the decision margin ($y * f(x) < 0$), the loss increases linearly with the negative value of $y * f(x)$, which encourages the SVM to correct the misclassification.

In the context of brain MRI images, the hinge loss serves as a critical component in determining an optimal hyperplane that effectively distinguishes between different classes of brain images, such as healthy versus abnormal or tumor regions. By minimizing the hinge loss, the Support Vector Machine (SVM) fine-tunes its hyperplane to balance maximizing the margin between classes and minimizing misclassifications. In essence, the hinge loss acts as a guiding principle during SVM training, penalizing misclassifications and playing a pivotal role in learning an effective decision boundary for binary classification tasks, which encompass brain MRI images. The comprehensive process of SVM, illustrated in

Figure 8, aims to establish a functional relationship between sample labels and data classification, facilitating accurate brain tumor detection. The decision function, integral to the classification of tumor and non-tumor regions, is a fundamental element of the feed-forward process in SVM classification and is mathematically represented as follows:

$$D(m) = \left(\sum_{i=1}^N \alpha_i y_i K(d_i m_i) + t \right). \quad (8)$$

In the equation 8, α_i represents the alpha coefficient associated with support vector class labels or feature vectors. The variables y_i denote the SVM vector, while d_i represents the input vector. Additionally, $K(d_i m_i)$ signifies the kernel function, which includes a bias term denoted as 't.'. The SVM-based brain tumor image classification process unfolds in three distinct steps. The initial step involves the selection of feature vectors through feature vector extraction. Subsequently, the second step encompasses the training of the data, and in the third step, the classification process is carried out to identify and delineate the tumor region.

The formation of the feature vector is achieved by aggregating data into an array, making it ready for the database processing that will eventually lead to object classification. In the context of brain tumor images, the process begins by converting the image into a binary representation, a transformation illustrated in Figure 9(a). Subsequently, the binary image undergoes skeletonization, as demonstrated in Figure 9(b). This processed image is divided into zones and areas, eventually combining to create the image matrix. The derived feature vector relies on various parameters, including Euler numbers and pixel distributions across the x and y planes. The outcome is a feature vector comprising around 100 distinct features, essential for accurately classifying brain tumor regions. In our work, we processed over 500 brain images for tumor classification. The SVM training leverages the feature vectors organized in a matrix format to classify tumor regions effectively. Support vectors in the SVM method represent the nearest data points to the decision surface. This assignment is a crucial aspect of brain tumor classification and involves an optimization process to determine the precise location on the surface corresponding to the region. SVM seeks to maximize the margin around the hyperplane separating classes, with the decision function relying on a subset of the training samples to identify the tumor region. The results of the SVM classification process are depicted in Figure 8.

Our proposed method effectively addresses the challenge of imbalanced segmentation in brain tumor detection, providing accurate results even when the tumor region is significantly smaller than the non-tumor regions. Figure 9 illustrates cases where brain tumors have notably smaller regions than non-tumor areas. Despite this imbalance, our proposed method demonstrates high accuracy in detecting these smaller tumor regions. Our approach could serve as a valuable clinical tool for tumor analysis, given its proficiency in handling imbalanced quantities and achieving precise

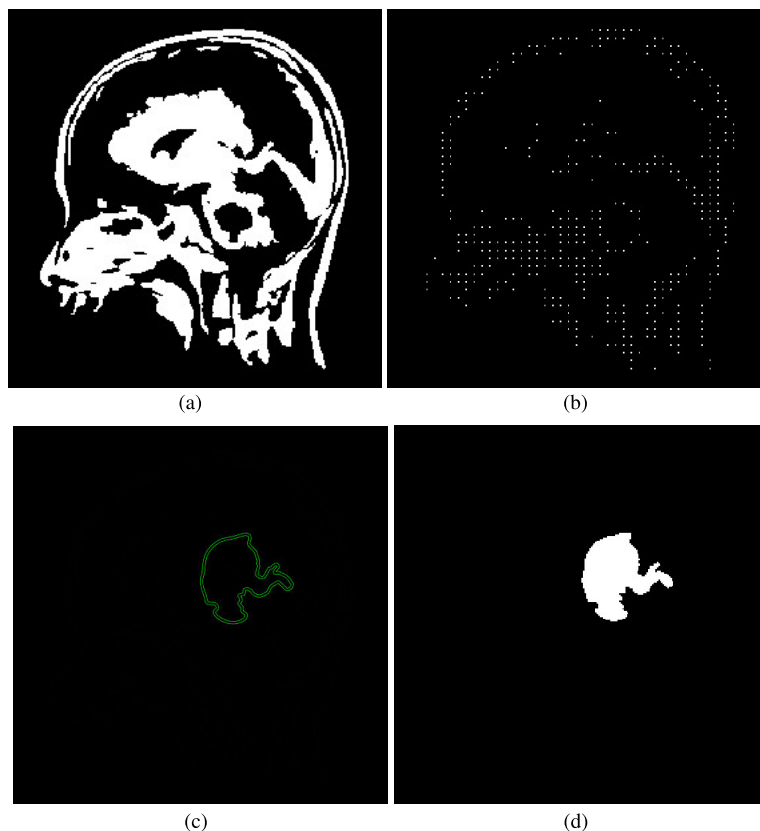


FIGURE 8. SVM-based classifier workflow for brain tumor detection. Figure (a): Binary representation of a brain image. Figure (b): Skeletonized image. Figure (c): SVM classifier applied to brain image. Figure (d): Detection of brain tumor regions.

segmentation—especially in scenarios where the tumor region is considerably smaller, presenting a challenging task.

F. COMPOSED ALGORITHM

The proposed algorithm excels in precisely identifying brain tumors while effectively addressing inherent challenges within brain MRI images. The sequential steps of the algorithm:

Step 01: Noise Reduction and Contrast Enhancement

- The algorithm recognizes the challenges associated with noise and inconsistent contrast in different brain regions of MRI images.
- Employing noise reduction techniques such as Wiener filtering, it tackles noise-related issues to improve image quality.
- The algorithm utilizes oriented diffusion filtering with Contrast-Limited Adaptive Histogram Equalization (CLAHE) to enhance contrast across diverse brain areas.
- These methods collectively constitute the “Enhancement Approach,” aimed at enhancing the overall quality of brain MRI images.

Step 2: Comprehensive Investigation of FCM and SVM Classification

- The algorithm’s impact on subsequent steps, particularly the FCM and SVM classification, is thoroughly examined.
- FCM is employed to accurately segment brain regions, leveraging the enhanced contrast achieved in the previous step.
- SVM classification further refines identifying tumor regions, benefiting from the improved image quality.

The algorithm follows a logical progression from noise reduction and contrast enhancement to precise segmentation and classification, ultimately proving its efficacy in addressing challenges specific to brain MRI images and accurately detecting brain tumors as culmination of algorithm is given below and The visual representation in Figure 10 further elucidates the interconnected steps of the algorithm.

Culmination of Composed Algorithm

- The workflow culminates by highlighting the algorithm’s adeptness in effectively addressing challenges related to noise and contrast within brain MRI images.
- The algorithm’s ability to accurately detect brain tumors is emphasized, showcasing its significance in medical image analysis.

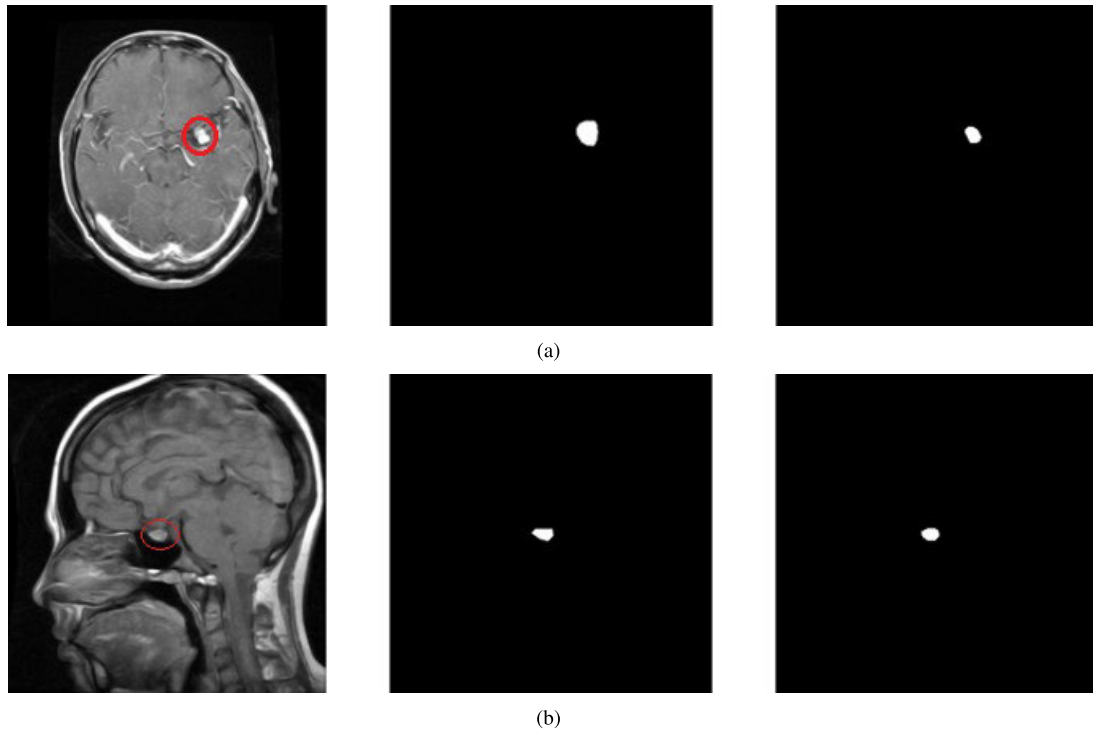


FIGURE 9. Illustration of brain tumor cases with notably smaller tumor regions, highlighted in red circles, compared to non-tumor areas. This emphasizes the precise detection achieved by our proposed method. The first column represents the original image, the second column displays the ground truth image, and the third column showcases the brain tumor detected through our proposed method.

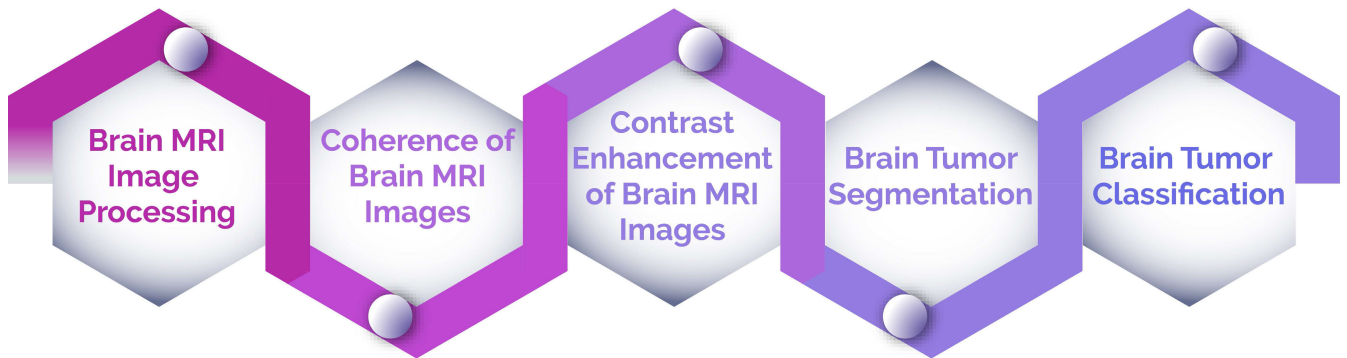


FIGURE 10. Enhanced Brain Tumor Detection Algorithm: A Comprehensive Workflow for Accurate Analysis of MRI Images.

- Empirical assessments affirm the algorithm’s superiority over existing brain tumor detection methods, reinforcing its reliability and effectiveness.

IV. DATABASE AND PARAMETERS MEASUREMENT

The proposed approach undergoes comprehensive evaluation, encompassing both the segmentation and classification of brain tumor regions. Segmentation performance is gauged through the analysis of six key parameters: mean, standard deviation, contrast, entropy, kurtosis, and skewness. In parallel, the classification of brain tumors is assessed based on sensitivity, specificity, and overall accuracy.

A. MEASURING PARAMETERS: SEGMENTATION OF BRAIN TUMOR

The performance of the segmentation results is assessed using six distinct parameters: mean, standard deviation, contrast, entropy, kurtosis, and skewness. Detailed explanations for each of these parameters can be found in [51].

B. MEASURING PARAMETERS: CLASSIFICATION OF BRAIN TUMOR

To measure the classification parameters, we conducted evaluations on both training and testing data. In order to thoroughly assess the database, we employed cross-

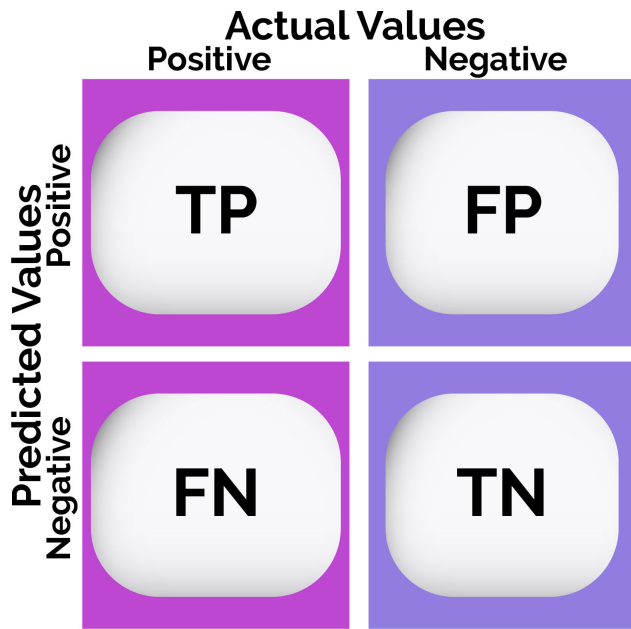


FIGURE 11. Visualization depicting the Performance Confusion Matrix of a Classification Model.

validation, a common technique for validating the performance of classification models. The following parameters were calculated for evaluating the classification model:

C. CONFUSION MATRIX

A confusion matrix serves as a structured table, offering a detailed summary of a classification model's performance on a specific dataset. It categorizes the model's predictions into four distinct outcomes: True Positives (TP), True Negatives (TN), False Positives (FP), and False Negatives (FN). Figure 11 provides an illustrative representation of the Confusion model.

The confusion matrix is a crucial tool for assessing a classification model's performance. It categorizes predictions into four outcomes: True Positives (correctly identified positives), True Negatives (correctly identified negatives), False Positives (incorrectly predicted positives), and False Negatives (missed positives). In medical imaging like brain MRI analysis, these components help evaluate the model's accuracy in detecting conditions, such as brain tumors. In medical imaging, particularly in brain MRI analysis, understanding these four outcomes is vital for computing key performance metrics, including sensitivity, specificity, and accuracy. These metrics play a crucial role in assessing the model's effectiveness in detecting conditions such as brain tumors, and their detailed explanations are provided below.

1) SENSITIVITY

Sensitivity (SN), also referred to as True Positive Rate (TPR) or Recall, is a performance metric that gauges the model's accuracy in correctly identifying positive instances. In the context of brain MRI images, sensitivity assesses the model's

capability to accurately detect genuine brain MRI pixels. Mathematically, sensitivity is determined as follows:

$$\text{Sensitivity (Se)} = TP / (TP + FN). \quad (9)$$

where: Sensitivity is a crucial metric in the evaluation of a classification model's performance, especially in medical imaging tasks like the analysis of brain MRI images. It can be explained by considering the two key components of the confusion matrix: True Positives (TP) and False Negatives (FN). TP represents the number of actual positive cases, such as diseased brain MRI images, that the model correctly identifies. On the other hand, FN represents the instances where the model misses or fails to identify actual positive cases. A higher sensitivity score indicates that the model excels at detecting the condition accurately, correctly identifying a larger proportion of true positive cases. This metric holds great significance in medical imaging applications where the primary objective is the precise detection and diagnosis of diseases, such as identifying brain tumors in MRI images. An elevated sensitivity value reflects the model's proficiency in minimizing the chances of missing potential cases, ultimately contributing to improved patient care and diagnostic accuracy.

2) SPECIFICITY

Specificity (SP), also known as True Negative Rate (TNR), is an essential metric for evaluating the performance of a classification model. In the realm of brain MRI image analysis, specificity assesses the model's capability to accurately identify negative instances, including false pixels. The mathematical expression for calculating specificity is as follows:

$$\text{Specificity} = TN / (TN + FP). \quad (10)$$

In the realm of medical diagnosis and specifically within the context of brain MRI images, the assessment of model performance revolves around two key components:

- **True Negatives (TN):** True negatives are the instances where the model accurately identifies non-cases, such as correctly recognizing healthy brain MRI images. TNs play a pivotal role in ensuring the model's capability to correctly classify cases where the condition is absent.
- **False Positives (FP):** In this particular scenario, false positives signify the instances where the model incorrectly categorizes non-cases as cases of the medical condition. Essentially, these are instances of false alarms.

Specificity emerges as a paramount metric, particularly in medical imaging and brain MRI analysis. It determines the model's proficiency in accurately identifying negative instances while endeavoring to minimize the occurrence of false positives. A higher specificity score underscores the model's effectiveness in distinguishing instances that do not exhibit the condition, a crucial aspect for reducing false alarms and maintaining the precision of medical diagnoses.

3) ACCURACY

Accuracy (AC) stands as a fundamental metric when it comes to assessing the comprehensive performance of a classification model, a principle that extends to applications involving brain MRI images. This pivotal metric quantifies the proportion of instances or pixels that the model has correctly predicted within the entire dataset. Mathematically, accuracy can be succinctly calculated through the following formula:

$$Accuracy = \frac{(TP + TN)}{(TP + TN + FP + FN)}. \quad (11)$$

In the realm of brain MRI images and medical diagnosis, these terms signify:

- TP: The number of positive cases correctly identified by the model.
- TN: The number of negative cases correctly identified by the model.
- FP: The number of negative cases incorrectly identified as positive by the model.
- FN: The number of positive cases incorrectly identified as negative by the model.

When accuracy is elevated, it signifies that the model adeptly and correctly classifies a larger proportion of both positive and negative pixels.

4) DICE SCORE

The Dice score (DSC) serves as a metric that illuminates the extent of overlap between the predicted output and the true ground truth values. It quantifies this overlap by normalizing the true positive values against the mean of the predicted and ground truth values. The mathematical representation of the Dice score is as follows:

$$DSC = \frac{2 \times TP}{(2 \times TN + FN + FP)}. \quad (12)$$

D. HAUSDORFF DISTANCE

Hausdorff distance (HD) is a mathematical metric used in brain MRI analysis to gauge the dissimilarity between segmented regions in different images, typically the region of interest in one image and its counterpart in another, known as the ground truth image. It assesses the accuracy of a segmentation algorithm by quantifying how well the segmented region aligns with the ground truth. A lower Hausdorff distance signifies better alignment, indicating more accurate segmentation that closely matches the actual shape and position of the region in the ground truth image. In applications like brain tumor detection, this spatial accuracy is crucial for precise diagnosis and treatment planning. HD is a key evaluation measure in brain MRI analysis, providing insights into the accuracy of segmentation algorithms.

The mathematical representation of the Hausdorff distance (HD) between two sets A and B (A represents the segmented brain tumor image set, and B is the ground truth image set) in a metric space is as follows:

Let A and B be two subsets of a metric space M with the distance function $d(x, y)$, where x and y are points in M . The directed Hausdorff distance from A to B , denoted $H(A, B)$, is defined as:

$$H(A, B) = \max [\min [d(a, b) : b \in B] : a \in A]. \quad (13)$$

In this equation:

- For each point a in set A , we calculate the minimum distance between a and any point in set B .
- Then, we take the maximum of these minimum distances on all set A points.

Similarly, the directed Hausdorff distance from B to A , denoted $H(B, A)$, is defined as follows:

$$H(B, A) = \max [\min [d(b, a) : a \in A] : b \in B]. \quad (14)$$

The symmetric Hausdorff distance between sets A and B , denoted $HD(A, B)$, is the maximum of the two directed Hausdorff distances:

$$HD(A, B) = \max [H(A, B), H(B, A)]. \quad (15)$$

In brain image analysis, A and B often represent the segmented region of interest in the test and ground truth images, respectively. The Hausdorff distance helps quantify the dissimilarity between these regions, providing a measure of precision for segmentation algorithms.

E. JACCARD SIMILARITY INDEX

The Jaccard Similarity Index (JSI), often referred to as Jaccard's Index or Coefficient, is a mathematical measure employed to evaluate the similarity between two sets by examining the ratio of their intersection to their union. When applied to brain MRI images, the Jaccard similarity index quantifies the level of overlap or concordance between two segmented regions, like brain tumor regions, in distinct images. Its mathematical definition is as follows:

Let A and B be two sets representing segmented regions of interest, such as brain tumor regions, in two brain MRI images.

- The intersection of sets A and B , denoted $|A \cap B|$, represents the number of elements (pixels) common to both sets. In the context of brain MRI images, this corresponds to the number of pixels that overlap between the two segmented regions.
- The union of sets A and B , denoted by $|A \cup B|$, represents the total number of combined elements (pixels) in the two sets. MRI images of the brain correspond to the total number of pixels in the two segmented regions.

The Jaccard Similarity Index (JSI) is then calculated as the ratio of the intersection of the sets to the union of the sets:

$$JSI(A, B) = |A \cap B| / |A \cup B|. \quad (16)$$

In the realm of medical imaging, including the analysis of brain MRI images, the Jaccard Similarity Index plays a crucial role in evaluating the precision of segmentation algorithms. A higher JSI value signifies a more substantial

overlap and resemblance between the segmented areas and the ground truth image, leading to more accurate segmentation. Conversely, a lower JSI value suggests less alignment and less precise segmentation.

In the specific context of brain MRI image analysis, a high Jaccard similarity index indicates that segmented tumor regions in different images are well-aligned, signifying accurate segmentation and a strong correspondence to the ground truth. The Jaccard similarity index, along with other metrics like the Dice score and Hausdorff distance, offers valuable insights into the performance of segmentation algorithms and their capability to faithfully represent regions of interest in brain MRI images.

F. DATABASES

When referring to a biological CE-MRI brain dataset, we allude to a compilation of images generated by applying contrast-enhanced magnetic resonance imaging (CE-MRI) techniques. These techniques are employed to investigate biological structures, and they involve the administration of contrast agents to augment the visibility of specific tissues or pathological conditions within MRI brain images during diagnostic procedures. Here are some key points about CE-MRI datasets and their potential applications:

- 1) The acquisition of CE-MRI datasets encompasses various imaging protocols, particularly contrast-enhanced T1-weighted sequences. These enhanced T1-weighted sequences enable the visualization and quantification of the distribution of the contrast agent in tissues over a specified time frame.
- 2) CE-MRI datasets are frequently gathered in the context of clinical trials for research purposes. They are often hosted in public repositories and research institutions, such as The Cancer Imaging Archive (TCIA) and the Alzheimer's Disease Neuroimaging Initiative (ADNI), which store MRI databases, including CE-MRI data, alongside other imaging modalities.
- 3) These datasets typically comprise 3D volumetric image sequences acquired at different time points following the administration of a contrast agent. They may consist of pre-contrast images, dynamic post-contrast series, and additional sequences for anatomical reference.
- 4) In brain tumor imaging, CE-MRI extensively evaluates brain tumors and delineates their boundaries. Contrast-enhanced sequences can highlight abnormal regions within brain MRI images, which indicate tumors. This functionality aids in diagnosing, planning, and monitoring treatment responses.
- 5) The dataset in question contains 3064 contrast-enhanced T1-weighted images obtained from 233 patients diagnosed with three different types of brain tumors: meningioma (708 slices), glioma (1426 slices), and pituitary tumors (930 slices) [53].
- 6) This dataset, called the CE-MRI Image Database [53], was compiled from Nanfang Hospital, Guangzhou,

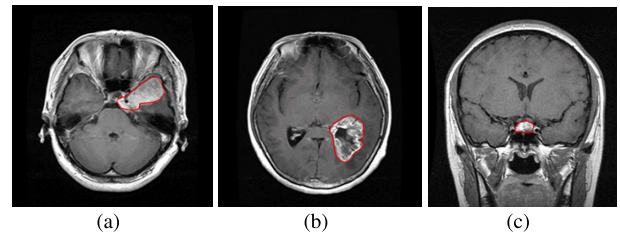


FIGURE 12. Celebrating Diversity: Brain Tumor Illustrations in CE-MRI Images: Fig (a) shows meningioma brain tumor. Fig (b) shows glioma brain tumor. Fig (c) shows pituitary brain tumor.

China, and General Hospital, Tianjin Medical University, China, from 2005 to 2010. It encompasses 3064 images from 233 patients, comprising 708 meningiomas, 1426 gliomas, and 930 pituitary tumors. These images have a resolution of 512×512 pixels with a pixel size of $0.49 \times 0.49 \text{mm}^2$ and a slice gap of 1mm . Data was split into 70% for training and 30% for testing. Three highly experienced radiologists manually identified the tumors in these images. Some sample images from the CE-MRI Image Database are displayed in Figure 12. This dataset is a valuable resource for research and development in brain tumor detection and analysis. It offers a diverse collection of images representing different types of brain tumors, facilitating the evaluation and improvement of medical imaging algorithms.

The standard reference to the biological characteristics of a CE-MRI brain dataset pertains to a collection of images acquired through the application of contrast-enhanced magnetic resonance imaging (CE-MRI) methodologies. CE-MRI entails the introduction of contrast agents to improve the visibility of specific tissues or pathological conditions in brain MRI scans during diagnostic procedures.

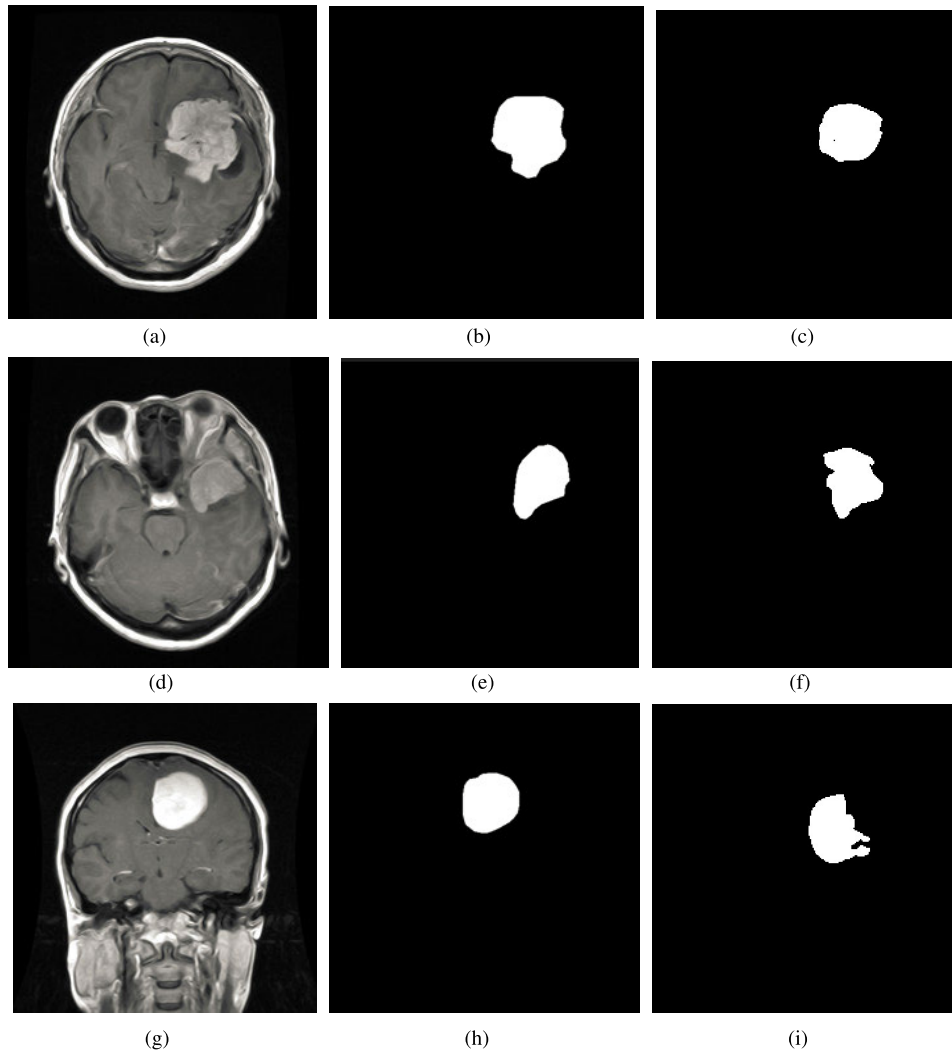
V. RESULTS ANALYSIS AND DISCUSSION

A. ANALYSIS OF SEGMENTATION MODULE PERFORMANCE

Various parameters are assessed to evaluate the performance of the brain tumor segmentation module using the CE-MRI database. The analysis is based on statistical metrics, as detailed in Table 1, which indicate optimal contrast throughout the region and enable accurate brain tumor segmentation. The image contrast (IC) of the proposed method's output has been significantly enhanced, with an IC value of 0.0299 recorded for the challenging pituitary tumor case. This result demonstrates substantial improvements in terms of uniformity and asymmetry measurements. The statistical analysis also demonstrates minimal pixel misclassifications or errors, resulting in precise tumor region segmentation, as visually depicted in Figure 13. The clear visualization of tumor detection underscores the efficacy of brain tumor detection.

TABLE 1. Performance analysis of Segmentation model of brain tumor.

Image Types	Mean	STD	IC	Entropy	Kurtosis	Skewness
Meningiomas Tumor Images	0.0046	0.090	0.30	3.19	35.20	5.84
Gliomas Tumor Images	0.0044	0.089	0.29	3.01	33.13	5.31
Pituitary Tumor Image	0.0041	0.084	0.29	3.01	32.92	5.26

**FIGURE 13.** Results of brain tumor segmentation using the proposed method. The first column displays images from the database, the second column shows the ground truth, and the third column illustrates the algorithm-generated output.

B. COMPARISON OF SEGMENTATION MODULE PERFORMANCE BASED ON DIFFERENT CLASSIFIER

Results of brain tumor segmentation using the proposed method is evaluated by measuring different parameters. As it is shown in the Figure 13, the first column displays images from the database, the second column shows the ground truth, and the third column illustrates the algorithm-generated output. Various researchers have employed different classifiers to segment brain tumors and have evaluated their performance using statistical metrics. These metrics

often include measures like mean, standard deviation (STD), image contrast (IC), and peak signal-to-noise ratio (PSNR). In Table 2, you can see a performance comparison of several classifiers, including K-Nearest Neighbor (KNN), Self-Organizing Map (SOM), Genetic Algorithm (GA), Graph Convolutional Neural Network (GCNN), Kernel-Based SVM, and our proposed approach (FCM-SVM). The results reveal that our proposed method surpasses existing techniques, underscoring its effectiveness in brain tumor detection and accurate tumor region classification. Further

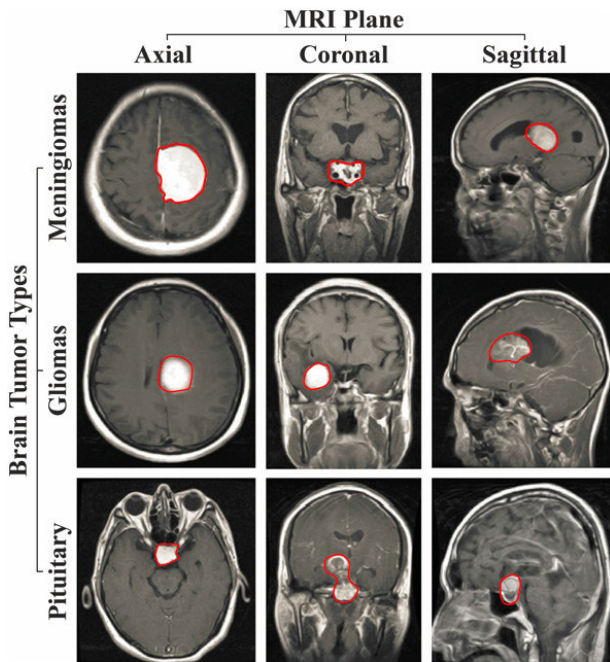


FIGURE 14. The representation of different tumor types in Brain MRI images.

details on the classification performance are provided in the following section.

C. ANALYSIS OF CLASSIFICATION MODULE PERFORMANCE

The assessment of the brain tumor classification module on the CE-MRI database involves scrutinizing various parameters. The Figure accompanying this information illustrates the representation of different tumor types in Brain MRI images. A comprehensive analysis of the classification model's performance is outlined in Table 3, with a specific focus on diverse brain tumor types, including meningiomas, gliomas, and pituitary tumors as shown in Figure 14. Please noted that statistical numbers of following parameters are averaged over multiple images of database.

The proposed method consistently exhibits robust predictive capabilities, as indicated by consistently high sensitivity and specificity values across all types of tumors. This performance is visually illustrated in the accompanying Figure 15. These elevated values affirm the model's proficiency in accurately identifying positive and negative cases, which is crucial for precise medical diagnoses. Additionally, noteworthy precision values reflect the overall accuracy of the model's predictions. However, it is imperative to delve into potential class imbalances and assess the clinical significance of these findings.

Dice score coefficients (DSC) indicate a substantial overlap between predicted and actual tumor regions, suggesting accurate segmentation. Nevertheless, in situations where minor discrepancies may have significant consequences, investigating the clinical implications of these overlaps

becomes necessary. Low Hausdorff distance (HD) values and Jaccard Index (JI) values further underscore the model's precise tumor segmentation, emphasizing its spatial accuracy and the degree of overlap between segmented and ground truth regions.

The effectiveness of the FCM-SVM classifier in accurately detecting abnormal tumor regions is verified through statistical parameter analysis. Essential metrics such as sensitivity, specificity, and accuracy are derived from the confusion matrix. Figure 16 illustrates the confusion matrix for randomly selected images of different brain tumor types, we took around 50 images of each classes of brain tumor images. The visual observation of brain tumor detection in different cases of brain tumors in MRI images, as depicted in the Figure 17, supports these findings. It indicates that our proposed method presents a promising approach for accurate and efficient brain tumor detection in medical applications.

D. COMPARISON OF CLASSIFICATION MODULE PERFORMANCE OF DIFFERENT CLASSIFIER

The presented Table 4 provides a comprehensive comparative analysis of various brain tumor detection methods, including the proposed method, based on performance metrics such as sensitivity, specificity, accuracy, Dice score (DSC), and processing time. Notably, the proposed method exhibits outstanding performance, achieving a sensitivity of 0.977, specificity of 0.979, accuracy of 0.982, and a DSC of 0.961. These metrics indicate a commendable balance between correctly identifying true positive and true negative cases, which is essential for accurate tumor detection and segmentation. Furthermore, the proposed method distinguishes itself with an efficient processing time of 0.42 seconds, underscoring its suitability for real-time or near-real-time applications. The proposed method consistently outperforms sensitivity and specificity compared to other methods, including traditional techniques like K-NN and more advanced approaches such as SVM, CNNs, and GANs. This suggests its efficacy in automating brain tumor detection through MRI analysis, offering a promising contribution to the field. However, it's essential to note that the absence of time information for some methods and the lack of performance metrics for others limit a comprehensive evaluation. Nonetheless, the proposed method emerges as a robust and efficient solution, showcasing its potential significance in advancing automated brain tumor diagnosis.

Our findings indicate that the proposed approach outperforms a majority of existing methods, demonstrating superior levels of sensitivity, specificity, accuracy, and Dice score. Furthermore, it highlights an expedited processing time when compared to certain models, emphasizing its capability for precise classification of tumor regions in brain imaging.

E. COMPARATIVE ANALYSIS WITH EXISTING WORK

To assess the effectiveness of our proposed method, we conducted a performance comparison with recent techniques developed from 2019 to the present, as depicted in Table 5.

TABLE 2. Comparison of Performance Segmentation model of brain tumor detection.

Method	Classifier	Mean	STD	IC	PSNR(dB)
Vrooman et al. [54]	K-NN	0.0032	0.071	0.19	0.75
Logeswari et al [28]	SOM	0.0028	0.067	0.18	0.76
Kharrat et al.[55]	GA	0.0033	0.074	0.21	0.78
Mamta et al.[56]	GCNN	0.0034	0.077	0.23	0.79
Mandle et al.[57]	Kernel-Based SVM	0.0031	0.072	0.22	0.98
Proposed Method	FCM-SVM	0.0042	0.085	0.28	1.1

TABLE 3. Performance analysis of Classification model of brain tumor. Note: S_e represent Sensitivity, S_p represent Specificity, A_c represent Accuracy.

Image Types	S_e	S_p	A_c	DSC	HD	JIS
Meningiomas Tumor Images	0.977	0.981	0.986	0.965	1.57	0.962
Gliomas Tumor Images	0.975	0.979	0.981	0.959	1.51	0.979
Pituitary Tumor Image	0.981	0.978	0.979	0.958	1.49	0.976
Overall Performance	0.977	0.979	0.982	0.961	1.52	0.972

TABLE 4. Comparison of Performance classification model of brain tumor detection with different classifier.

method	Sensitivity	Specificity	Accuracy	DSC	Time
K-NN [54]	0.39	0.42	0.85	0.81	3.7s
SOM [28]	0.43	0.52	0.92	0.83	4.8s
GA [55]	0.51	0.54	0.98	0.85	2.8s
GCNN [56]	0.85	0.89	0.96	0.89	0.92s
Kernel-Based SVM [57]	0.98	0.98	0.98	0.94	0.83s
SVM [58]	-	-	0.96	-	-
BP-NN [59]	-	-	0.93	-	-
DWA-DNN[60]	-	-	0.96	-	-
GANs [61]	-	-	0.91	-	-
CNN [62]	-	-	0.91	-	-
CNN [63]	-	-	0.96	-	-
K-NN [64]	-	-	0.86	-	-
Deep LSTM [65]	-	-	0.97	-	-
FCM [66]	-	-	0.97	-	-
SVM[67]	-	-	0.99	-	-
CNN [68]	-	-	0.97	-	-
CNN [69]	-	-	0.92	-	-
EL-FCM [70]	-	-	0.99	-	-
CNN [71]	-	-	0.95	-	-
SVM [72]	-	-	0.95	-	-
SVM [73]	-	-	0.95	-	-
DenseNet [74]	0.95	0.94	0.94	-	-
VGG19 [75]	0.95	0.95	0.94	-	-
SVM [76]	0.96	0.96	0.97	-	-
Proposed Method	0.977	0.979	0.982	0.961	0.42s

Our method exhibited relatively superior performance when compared to existing classifiers. It is worth noting that despite the emergence of more CNN or deep learning-based methods since 2019, their performance remains comparatively modest

due to the absence of groundbreaking processing methods. In contrast, our proposed method, which is rooted in FCM-SVM and advanced techniques, surpassed many other methods due to the enhanced coherence among diverse

TABLE 5. Performance of exiting MR imaging segmentation methods.

Method	Year	Technique	Ac (%)
[58]	2017	SVM	96.51
[43]	2018	Capsule Networks (CapsNet)	95.03
[77]	2018	Extreme Learning Machines (ELM)	93.68
[78]	2019	Regularized Extreme Learning Machine	92.61
[79]	2019	Convolution Neural Networks (CNNs)	96.13
[59]	2019	Back propagation neural networks.	93.33
[60]	2019	Deep Wavelet Autoencoder (DWA) and Deep Neural Network (DNN).	96
[61]	2019	Generative Adversarial Networks (GANs)	91
[62]	2019	Convolutional neural network	91.2
[63]	2019	Convolutional neural network	97.87
[64]	2019	K-NN	86
[65]	2019	Deep LSTM	97.87
[66]	2019	FCM clustering algorithm	97.5
[67]	2019	SVM	99.8
[68]	2019	KM-FCM	97
[69]	2019	Convolutional Neural Network	92
[70]	2019	Convolutional Neural Network	99.34
[71]	2020	Extreme learning based on FCM	95
[72]	2020	convolutional Neural Network	95
[73]	2022	SVM	95.1
[80]	2023	Ensemble of Deep Learning Model	97.7
Proposed Method	2023	Contrast Normalization Techniques and SVM	98.2

brain MRI image regions, resulting in an improved classifier performance. Our forthcoming research will center on the development of innovative techniques that harness machine learning to augment training data, ultimately aiming to outperform existing methods.

F. DISCUSSION ON PERFORMANCE OF PROPOSED METHOD

The outcomes of the proposed pipeline demonstrate significant enhancements in various aspects when classifying meningioma versus pituitary tumors compared to existing methods. Here's a breakdown of the achieved performance based on each parameter:

- An average sensitivity of 0.981 indicates a high success rate in accurately identifying pituitary tumors.
- A specificity of 0.981 suggests the method's effectiveness in distinguishing pituitary tumors from meningioma tumors.
- With an accuracy value of 0.982, the method exhibits high precision in correctly identifying meningioma tumors without misclassifying pituitary tumors.
- A Dice Similarity Coefficient (DSC) of 0.961 demonstrates substantial agreement between the proposed method's classifications and the actual tumor locations, indicating high accuracy.
- Notably, the proposed method boasts a shorter execution time of 0.42 seconds compared to existing works, signifying efficiency and computational speed.

Overall, the results imply that the proposed method surpasses existing sensitivity, specificity, accuracy, and DSC techniques. These improvements hold great promise in medical imaging, potentially leading to more precise and efficient diagnoses. This, in turn, can expedite treatment decisions for patients with meningioma and pituitary tumors, ultimately enhancing their care.

VI. STRENGTHS AND LIMITATIONS: A COMPREHENSIVE ANALYSIS

The suggested approach has its merits and drawbacks, with the strengths outlined below.

- A standout feature of the study is the introduction of a sophisticated automated segmentation pipeline. This novel approach integrates advanced preprocessing techniques, such as contrast-limited adaptive histogram equalization (CLAHE) and diffusion filtering, streamlining the segmentation and classification of brain tumors in MRI images to potentially enhance accuracy.
- The incorporation of the Fuzzy C-Means (FCM) algorithm for segmentation is a noteworthy strength. Recognized for its efficacy in delineating structures in medical images, FCM contributes to improved accuracy in identifying abnormal regions related to brain tumors. However, the sensitivity of FCM to outliers and noise necessitates caution. To address this, hybrid approaches were implemented, combining FCM with other methods or incorporating additional preprocessing

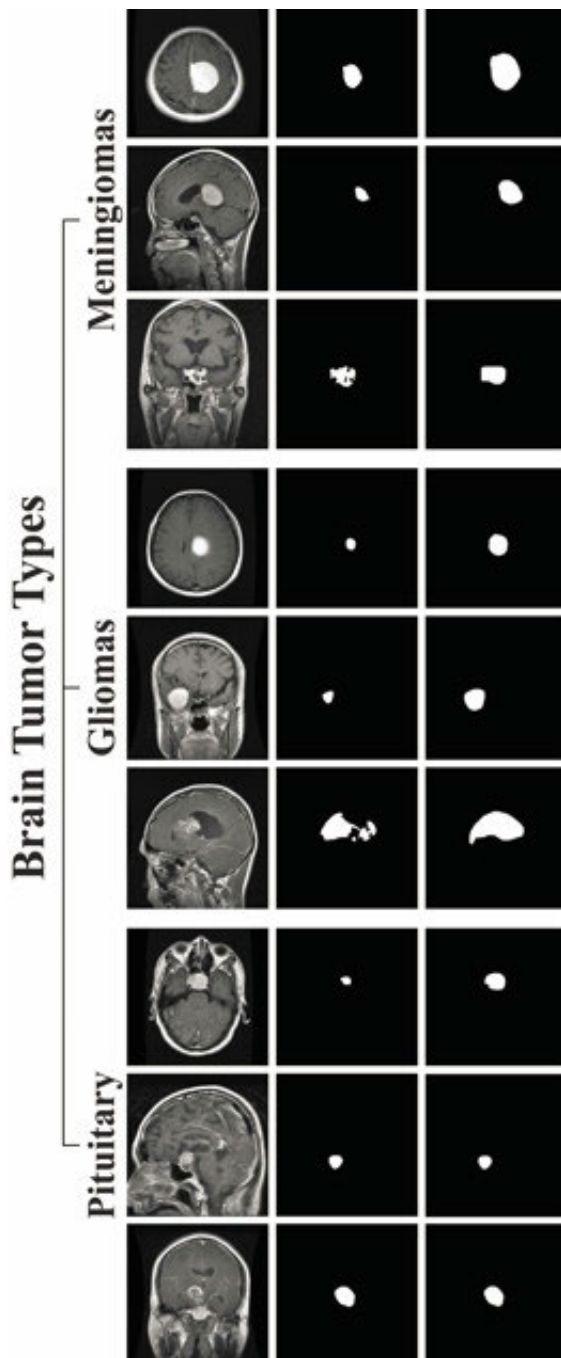


FIGURE 15. Visual representation of brain tumor segmentation across diverse brain types. The first column displays brain MRI images, the second column exhibits ground truth images, and the third column showcases the segmented output images.

steps to enhance segmentation accuracy, particularly in datasets with noise or outliers.

- The incorporation of a Support Vector Machine (SVM) classifier enhances the proposed method's ability to handle complex classification tasks, leveraging the effectiveness of SVMs in machine learning applications with intricate decision boundaries.

- The study demonstrates strength in a comprehensive evaluation, utilizing a Contrast-Enhanced Magnetic Resonance Imaging (CE-MRI) database that includes various brain tumor types. This approach ensures the robustness and generalizability of the proposed method.
- The proposed method showcases superior performance metrics, including high sensitivity, specificity, accuracy, and Dice Score (DSC). These metrics collectively affirm the method's proficiency in precisely identifying and classifying brain tumor regions, marking a significant strength.
- The methodology boasts a notably shorter processing time of 0.41 seconds, a crucial aspect for practical implementation in clinical settings where timely diagnosis is imperative. This efficiency stands out as a notable strength compared to conventional approaches, adding a novel dimension to the proposed methodology.

Despite the promising results demonstrated by the proposed MRI-based automated brain tumor segmentation and classification method, it is imperative to acknowledge its inherent limitations:

- **Limited Generalization:** The method's optimized performance on the specific CE-MRI database used for testing may not seamlessly generalize to diverse datasets or populations, presenting challenges that will be addressed in future implementations.
- **Dependency on Image Quality:** The efficacy of the proposed method is susceptible to variations in the quality of input MRI images, where artifacts, poor resolution, or other quality issues may compromise segmentation and classification accuracy. The validation of preprocessing on extensive databases is essential to enhance performance and plays a pivotal role in refining future brain tumor methodologies.
- **Sensitivity to Parameter Settings:** The Fuzzy C-Means (FCM) clustering technique and Support Vector Machine (SVM) classifier's performance may be sensitive to parameter settings, requiring careful tuning as optimal parameters for one dataset may not be directly applicable to others. Selecting optimal parameters through validation on a large database becomes crucial for effective clustering.
- **Lack of Clinical Validation:** The proposed method lacks validation in a large-scale clinical setting, posing a potential gap in ensuring its reliability and safety in real-world scenarios.
- **Future Data Drift and Updates:** The method's efficacy may diminish over time due to evolving imaging technology, changes in clinical practices, or the availability of new datasets. Regular updates and adaptation to emerging trends in medical imaging are essential to maintain relevance.

Addressing these limitations through ongoing research, particularly in diverse clinical settings, will contribute

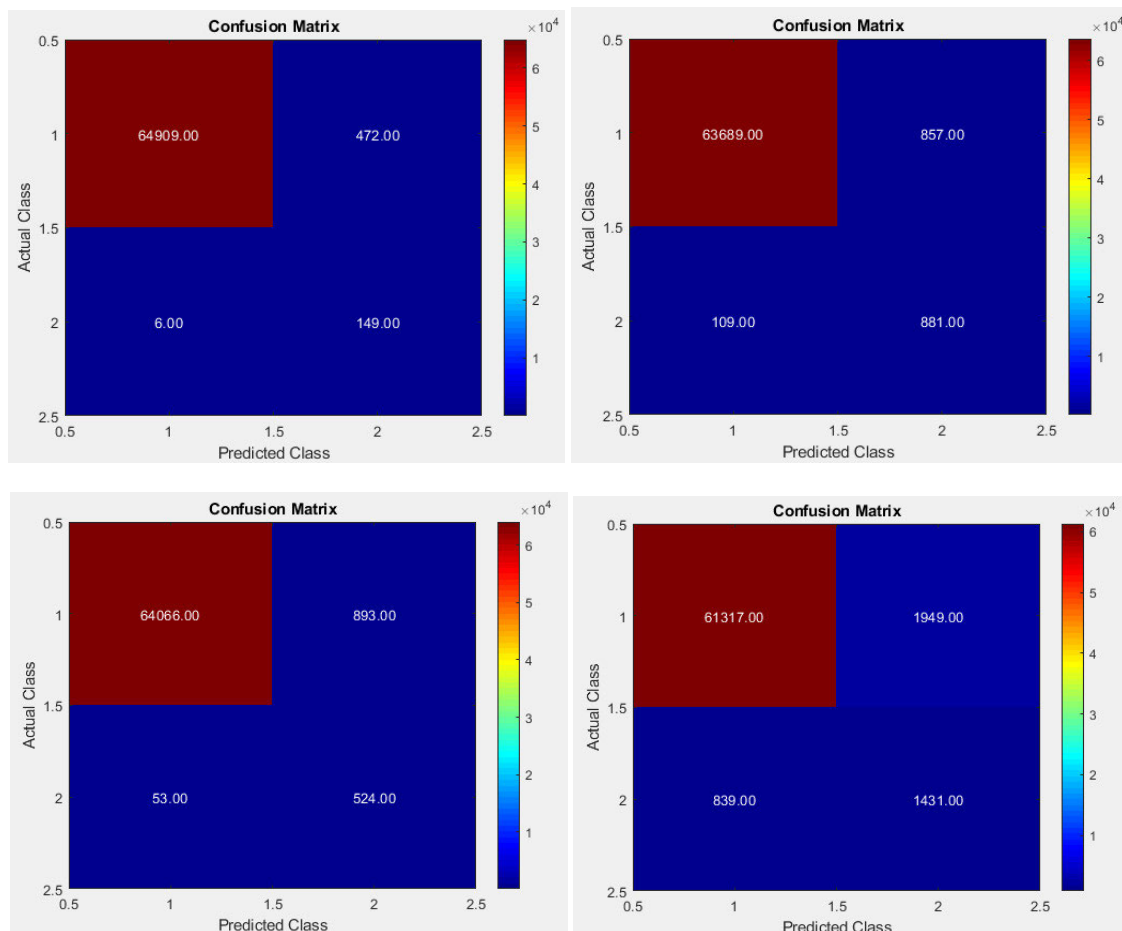


FIGURE 16. Confusion Matrix of randomly selected Images sets of brain different brain tumor types.

significantly to fortifying the robustness and real-world applicability of the proposed method.

VII. CONCLUSION AND FUTURE DIRECTION

This research presents a comprehensive pipeline for the automated segmentation and classification of brain tumors. The proposed method stands as a testament to innovation and efficacy in brain tumor detection. Our method introduces unique modifications in each step, emphasizing its innovative nature. The true essence of its uniqueness lies in the meticulous combination and adaptation of these techniques, specifically tailored to address the intricacies of magnetic resonance (MR) images. By carefully selecting and integrating established methodologies, we have made deliberate adjustments to optimize their performance, acknowledging and addressing the challenges presented by MR images. Notably, our method introduces a novel framework with innovative preprocessing techniques like contrast-limited adaptive histogram equalization (CLAHE) and diffusion filtering, enhancing and coalescing MR brain images to suit the specific characteristics of MR imaging. Including the Fuzzy C-Means (FCM) algorithm for segmentation and integrating a Support Vector Machine (SVM) classifier

further contributes to the uniqueness of our approach. The selection of two clusters in FCM, one representing the background image and the other encompassing the brain area, including tumors, is a pivotal contribution. This integration, coupled with SVM, successfully overcomes over-segmentation issues, improving performance. Our method employs coherent filtering and novel contrast adjustments, producing a well-uniform contrast image with minimal noise.

Moreover, our proposed pipeline undergoes a comprehensive evaluation using a Contrast-Enhanced Magnetic Resonance Imaging (CE-MRI) database covering diverse brain tumor types. The performance metrics, including sensitivity, specificity, accuracy, and Dice Score (DSC), demonstrate the proficiency of our method in precisely identifying and classifying brain tumor regions. Notably, its efficient processing time of only 0.42 seconds underscores its practical viability in clinical settings.

Numerous opportunities for further enhancement and expansion have been identified for future work. Standardizing the pipeline through ensemble techniques and machine learning innovations can enhance robustness. Additionally, integrating deep learning methods, such as convolutional neural networks (CNNs), holds promise for further accuracy

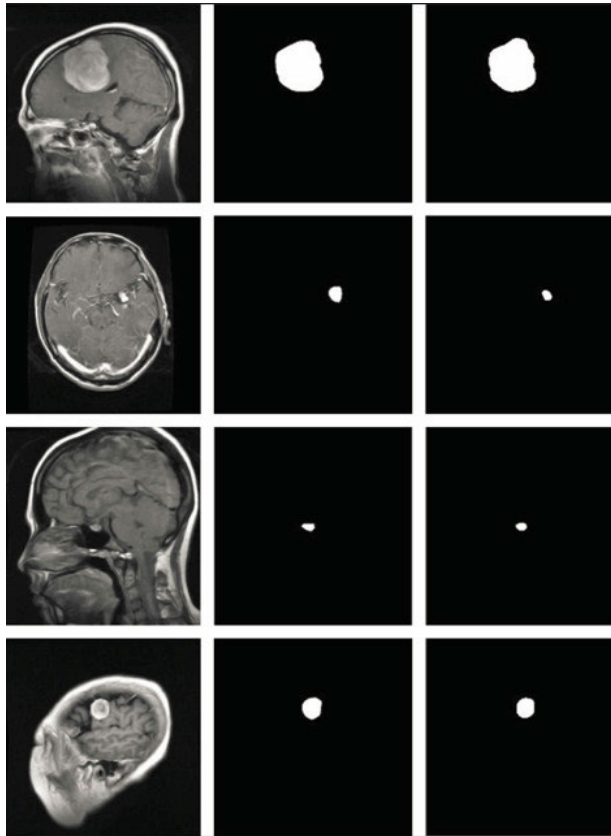


FIGURE 17. The figure provides a scrutiny of brain tumor detection across various types from distinct MRI planes, with each image presenting its own set of challenges. In the first column, original images containing brain tumors are presented, showcasing diverse tumor locations. The second column exhibits the corresponding ground truth images, and the third column highlights the results produced by our proposed method.

gains. Including a larger and more diverse dataset and multimodal image analysis is essential to improving generalizability. Validation studies, real-time applications, and integration with clinical decision support systems represent promising avenues for future research, fostering advances in automated brain tumor analysis.

Collectively, these improvements enhance the diagnostic process and pave the way for more accurate and efficient brain tumor diagnosis, benefitting patients by enabling timely and well-informed treatment decisions. The significance of this research lies in its potential to contribute to the development of state-of-the-art medical imaging tools with tangible impacts on patient care and outcomes. Our method introduces significant adaptations and innovations, showcasing its effectiveness in automated brain tumor diagnosis. This approach marks a noteworthy advancement over conventional methods, offering a promising avenue for accurate and efficient brain tumor detection in medical applications.

REFERENCES

- [1] A. K. Budati and R. B. Katta, "An automated brain tumor detection and classification from MRI images using machine learning techniques with IoT," *Environ., Develop. Sustainability*, vol. 24, no. 9, pp. 10570–10584, Sep. 2022.
- [2] Z. Yao, Z. Zhang, and L.-Q. Xu, "Convolutional neural network for retinal blood vessel segmentation," in *Proc. 9th Int. Symp. Comput. Intell. Design (ISCID)*, vol. 1, Dec. 2016, pp. 406–409.
- [3] T. Armstrong, M. Cohen, J. Weinberg, and M. Gilbert, "Imaging techniques in neuro-oncology," *Seminars Oncol. Nursing*, vol. 20, no. 4, pp. 231–239, Nov. 2004.
- [4] H. W. Kim, L. Van Assche, R. B. Jennings, W. B. Wince, C. J. Jensen, W. G. Rehwald, D. C. Wendell, L. Bhatti, D. M. Spatz, M. A. Parker, E. R. Jenista, I. Klem, A. L. C. Crowley, E.-L. Chen, R. M. Judd, and R. J. Kim, "Relationship of T2-weighted MRI myocardial hyperintensity and the ischemic area-at-risk," *Circulat. Res.*, vol. 117, no. 3, pp. 254–265, Jul. 2015.
- [5] W. Deng, Q. Shi, K. Luo, Y. Yang, and N. Ning, "Brain tumor segmentation based on improved convolutional neural network in combination with non-quantifiable local texture feature," *J. Med. Syst.*, vol. 43, no. 6, pp. 1–9, Jun. 2019.
- [6] K. R. Babu, P. V. Nagajanyulu, and K. S. Prasad, "Brain tumor segmentation of T1w MRI images based on clustering using dimensionality reduction random projection technique," *Current Med. Imag. Formerly Current Med. Imag. Rev.*, vol. 17, no. 3, pp. 331–341, Apr. 2021.
- [7] N. D. Indira, K. R. Babu, M. A. Kumar, D. S. Kiran, and D. P. Sashank, "Brain tumor detection from MRI images using optimization segmentation techniques," *Int. J. Adv. Sci. Technol.*, vol. 29, no. 4, pp. 7858–7865, 2020.
- [8] A. Lundervold and A. Lundervold, "An overview of deep learning in medical imaging focusing on MRI," *J. Med. Phys.*, vol. 29, no. 2, pp. 102–127, 2019.
- [9] Y. Jiang, J. Hou, X. Xiao, and H. Deng, "A brain tumor segmentation new method based on statistical thresholding and multiscale CNN," in *Proc. Int. Conf. Intell. Comput.*, 2018, pp. 235–245.
- [10] M. Hssayeni, "Computed tomography images for intracranial hemorrhage detection and segmentation," (version 1.3.1), *PhysioNet*, 2020, doi: 10.13026/4nae-zg36.
- [11] K. K. G. R. Babu, K. K. M. Prasad, K. R. Krishna, M. G. Samhith, and P. J. Pushpitha, "Effective detection of brain tumour on MRI images using optimization based segmentation techniques," *Int. J. Sci. Technol. Res.*, vol. 9, no. 1, pp. 1182–1185, 2020.
- [12] E. F. Badran, E. G. Mahmoud, and N. Hamdy, "An algorithm for detecting brain tumors in MRI images," in *Proc. Int. Conf. Comput. Eng. Syst.*, Nov. 2010, pp. 368–373.
- [13] S. Shameem K. R. Babu, U. S. Deepthi, A. S. Madhuri, and P. S. Prasad, "Comparative analysis of brain tumor detection using deep learning methods," *Int. J. Sci. Technol. Res.*, vol. 8, no. 12, pp. 252–254, 2019.
- [14] J. Nodirov, A. B. Abdusalomov, and T. K. Whangbo, "Attention 3D U-Net with multiple skip connections for segmentation of brain tumor images," *Sensors*, vol. 22, no. 17, p. 6501, Aug. 2022.
- [15] A. S. M. Shafi, M. B. Rahman, T. Anwar, R. S. Halder, and H. M. E. Kays, "Classification of brain tumors and auto-immune disease using ensemble learning," *Informat. Med. Unlocked*, vol. 24, Jan. 2021, Art. no. 100608.
- [16] S. Pereira, A. Pinto, V. Alves, and C. A. Silva, "Brain tumor segmentation using convolutional neural networks in MRI images," *IEEE Trans. Med. Imag.*, vol. 35, no. 5, pp. 1240–1251, May 2016.
- [17] S. Ahuja, B. K. Panigrahi, and T. K. Gandhi, "Enhanced performance of dark-nets for brain tumor classification and segmentation using colormap-based superpixel techniques," *Mach. Learn. With Appl.*, vol. 7, Mar. 2022, Art. no. 100212.
- [18] Y. Lecun, L. Bottou, Y. Bengio, and P. Haffner, "Gradient-based learning applied to document recognition," *Proc. IEEE*, vol. 86, no. 11, pp. 2278–2324, Nov. 1998.
- [19] V. Badrinarayanan, A. Kendall, and R. Cipolla, "SegNet: A deep convolutional encoder–decoder architecture for image segmentation," *IEEE Trans. Pattern Anal. Mach. Intell.*, vol. 39, no. 12, pp. 2481–2495, Dec. 2017.
- [20] A. Krizhevsky, I. Sutskever, and G. E. Hinton, "ImageNet classification with deep convolutional neural networks," *Commun. ACM*, vol. 60, no. 6, pp. 84–90, May 2017.
- [21] J. Cheng, W. Huang, S. Cao, R. Yang, W. Yang, Z. Yun, Z. Wang, and Q. Feng, "Enhanced performance of brain tumor classification via tumor region augmentation and partition," *PLoS ONE*, vol. 10, no. 10, Oct. 2015, Art. no. e0140381.
- [22] M. A. Al-antari, M. A. Al-masni, M.-T. Choi, S.-M. Han, and T.-S. Kim, "A fully integrated computer-aided diagnosis system for digital X-ray mammograms via deep learning detection, segmentation, and classification," *Int. J. Med. Informat.*, vol. 117, pp. 44–54, Sep. 2018.

- [23] M. A. Mazurowski, M. Buda, A. Saha, and M. R. Bashir, "Deep learning in radiology: An overview of the concepts and a survey of the state of the art with focus on MRI," *J. Magn. Reson. Imag.*, vol. 49, no. 4, pp. 939–954, Apr. 2019.
- [24] A. Isin, C. D. Glu, and M. Sah, "Review of MRI-based brain tumor image segmentation using deep learning methods," *Proc. Comput. Sci.*, vol. 102, pp. 317–324, Jan. 2016.
- [25] A. Kazemi, M. E. Shiri, A. Sheikahmadi, and M. Khodamoradi, "Classifying tumor brain images using parallel deep learning algorithms," *Comput. Biol. Med.*, vol. 148, Sep. 2022, Art. no. 105775.
- [26] X. Zhao, Y. Wu, G. Song, Z. Li, Y. Zhang, and Y. Fan, "A deep learning model integrating FCNNs and CRFs for brain tumor segmentation," *Med. Image Anal.*, vol. 43, pp. 98–111, Jan. 2018.
- [27] T. A. Soomro, L. Zheng, A. J. Afifi, A. Ali, S. Soomro, M. Yin, and J. Gao, "Image segmentation for MR brain tumor detection using machine learning: A review," *IEEE Rev. Biomed. Eng.*, vol. 16, pp. 70–90, 2023.
- [28] T. Logeswari and M. Karnan, "An improved implementation of brain tumor detection using segmentation based on hierarchical self organizing map," *Int. J. Comput. Theory Eng.*, vol. 2, no. 4, pp. 591–595, 2010.
- [29] M. Lather and P. Singh, "Investigating brain tumor segmentation and detection techniques," *Proc. Comput. Sci.*, vol. 167, pp. 121–130, Jan. 2020.
- [30] K. V. Chaithanyadas and G. R. G. King, "Brain tumour classification: A comprehensive systematic review on various constraints," *Comput. Methods Biomechanics Biomed. Eng., Imag. Visualizat.*, vol. 11, no. 3, pp. 517–529, May 2023.
- [31] B. Yin, C. Wang, and F. Abza, "New brain tumor classification method based on an improved version of whale optimization algorithm," *Biomed. Signal Process. Control*, vol. 56, Feb. 2020, Art. no. 101728.
- [32] S. Alagarsamy, K. Kamatchi, V. Govindaraj, Y.-D. Zhang, and A. Thiagarajan, "Multi-channelled MR brain image segmentation: A new automated approach combining BAT and clustering technique for better identification of heterogeneous tumors," *Biocybernetics Biomed. Eng.*, vol. 39, no. 4, pp. 1005–1035, Oct. 2019.
- [33] A. Kumar, M. Ramachandran, A. H. Gandomi, R. Patan, S. Lukasiak, and R. K. Soundarapandian, "A deep neural network based classifier for brain tumor diagnosis," *Appl. Soft Comput.*, vol. 82, Sep. 2019, Art. no. 105528.
- [34] F. Özyurt, E. Sert, E. Avci, and E. Dogantekin, "Brain tumor detection based on convolutional neural network with neurosophic expert maximum fuzzy sure entropy," *Measurement*, vol. 147, Dec. 2019, Art. no. 106830.
- [35] A. Selvapandian and K. Manivannan, "Fusion based glioma brain tumor detection and segmentation using ANFIS classification," *Comput. Methods Programs Biomed.*, vol. 166, pp. 33–38, Nov. 2018.
- [36] M. Sharif, J. Amin, M. Raza, M. Yasmin, and S. C. Satapathy, "An integrated design of particle swarm optimization (PSO) with fusion of features for detection of brain tumor," *Pattern Recognit. Lett.*, vol. 129, pp. 150–157, Jan. 2020.
- [37] M. Sharma, G. N. Purohit, and S. Mukherjee, "Information retrieves from brain MRI images for tumor detection using hybrid technique K-means and artificial neural network (KMANN)," in *Networking Communication and Data Knowledge Engineering*, vol. 4. Singapore: Springer, 2018.
- [38] N. V. Shree and T. N. R. Kumar, "Identification and classification of brain tumor MRI images with feature extraction using DWT and probabilistic neural network," *Brain Informat.*, vol. 5, no. 1, pp. 23–30, Mar. 2018.
- [39] A. R. Raju, P. Suresh, and R. R. Rao, "Bayesian HCS-based multi-SVNN: A classification approach for brain tumor segmentation and classification using Bayesian fuzzy clustering," *Biocybernetics Biomed. Eng.*, vol. 38, no. 3, pp. 646–660, 2018.
- [40] M. K. Abd-Ellah, A. I. Awad, A. A. M. Khalaf, and H. F. A. Hamed, "Two-phase multi-model automatic brain tumour diagnosis system from magnetic resonance images using convolutional neural networks," *EURASIP J. Image Video Process.*, vol. 2018, no. 1, pp. 1–10, Dec. 2018.
- [41] R. Rani and A. Kamboj, "Brain tumor classification for MR imaging using support vector machine," in *Progress in Advanced Computing and Intelligent Engineering*, vol. 2. Cham, Switzerland: Springer, 2019.
- [42] R. Torres-Molina, C. Bustamante-Orellana, A. Riofrío-Valdivieso, F. Quinga-Socasi, R. Guachi, and L. Guachi-Guachi, "Brain tumor classification using principal component analysis and kernel support vector machine," in *Intelligent Data Engineering and Automated Learning IDEAL 2019*, Manchester, U.K. Cham, Switzerland: Springer, Nov. 2019, pp. 89–96.
- [43] S. Samarath R. Phaye, A. Sikka, A. Dhali, and D. Bathula, "Dense and diverse capsule networks: Making the capsules learn better," 2018, *arXiv:1805.04001*.
- [44] J. S. Paul, A. J. Plassard, B. A. Landman, and D. Fabbri, "Deep learning for brain tumor classification," *Proc. SPIE*, vol. 10137, Mar. 2017, Art. no. 1013710.
- [45] M. Arabahmadi, R. Farahbakhsh, and J. Rezazadeh, "Deep learning for smart healthcare—A survey on brain tumor detection from medical imaging," *Sensors*, vol. 22, no. 5, p. 1960, Mar. 2022.
- [46] T. A. Soomro, A. Ali, N. A. Jandan, A. J. Afifi, M. Irfan, S. Alqhtani, A. Glowacz, A. Alqhtani, R. Tadeusiewicz, E. Kantoch, and L. Zheng, "Impact of novel image preprocessing techniques on retinal vessel segmentation," *Electronics*, vol. 10, no. 18, p. 2297, Sep. 2021.
- [47] C. Gottschlich and C.-B. Schonlieb, "Oriented diffusion filtering for enhancing low-quality fingerprint images," *IET Biometrics*, vol. 1, no. 2, pp. 105–113, Jun. 2012.
- [48] G. T. Mgbejime, M. A. Hossin, G. U. Nneji, H. N. Monday, and F. Ekong, "Parallelistic convolution neural network approach for brain tumor diagnosis," *Diagnostics*, vol. 12, no. 10, p. 2484, Oct. 2022.
- [49] J. A. Sethian, "Fast marching methods," *SIAM Rev.*, vol. 41, no. 2, pp. 199–235, Jan. 1999.
- [50] R. Vankdothu and M. A. Hameed, "Brain tumor segmentation of MR images using SVM and fuzzy classifier in machine learning," *Measurement, Sensors*, vol. 24, Dec. 2022, Art. no. 100440.
- [51] Y. E. Almalki, N. A. Jandan, T. A. Soomro, A. Ali, P. Kumar, M. Irfan, M. U. Keerio, S. Rahman, A. Alqhtani, S. M. Alqhtani, M. A. M. Hakami, W. A. Aldhabaan, and A. S. Khairallah, "Enhancement of medical images through an iterative McCann retinex algorithm: A case of detecting brain tumor and retinal vessel segmentation," *Appl. Sci.*, vol. 12, no. 16, p. 8243, Aug. 2022.
- [52] S. A. Saeed, T. A. Soomro, N. A. Jandan, A. Ali, M. Irfan, S. Rahman, W. A. Aldhabaan, A. S. Khairallah, and I. Abuallat, "Impact of retinal vessel image coherence on retinal blood vessel segmentation," *Electronics*, vol. 12, no. 2, p. 396, Jan. 2023.
- [53] J. Cheng, *Brain Tumor Dataset*. London, U.K.: Figshare. Dataset, 2017.
- [54] H. A. Vrooman, C. A. Cocosco, F. van der Lijn, R. Stokking, M. A. Ikram, M. W. Vernooij, M. M. B. Breteler, and W. J. Niessen, "Multi-spectral brain tissue segmentation using automatically trained k-nearest-neighbor classification," *NeuroImage*, vol. 37, no. 1, pp. 71–81, Aug. 2007.
- [55] A. Kharrat et al., "A hybrid approach for automatic classification of brain MRI using genetic algorithm and support vector machine," *Leonardo J. Sci.*, vol. 9, pp. 71–82, 2010.
- [56] M. Mittal, L. M. Goyal, S. Kaur, I. Kaur, A. Verma, and D. Jude Hemanth, "Deep learning based enhanced tumor segmentation approach for MR brain images," *Appl. Soft Comput.*, vol. 78, pp. 346–354, May 2019.
- [57] A. K. Mandle, S. P. Sahu, and G. Gupta, "Brain tumor segmentation and classification in MRI using clustering and kernel-based SVM," *Biomed. Pharmacol. J.*, vol. 15, no. 2, pp. 699–716, Jun. 2022.
- [58] N. B. Bahadure, A. K. Ray, and H. P. Thethi, "Image analysis for MRI based brain tumor detection and feature extraction using biologically inspired BWT and SVM," *Int. J. Biomed. Imag.*, vol. 2017, pp. 1–12, Apr. 2017.
- [59] P. M. Shakeel, T. E. El. Tobely, H. Al-Feel, G. Manogaran, and S. Baskar, "Neural network based brain tumor detection using wireless infrared imaging sensor," *IEEE Access*, vol. 7, pp. 5577–5588, 2019.
- [60] P. K. Mallick, S. H. Ryu, S. K. Satapathy, S. Mishra, G. N. Nguyen, and P. Tiwari, "Brain MRI image classification for cancer detection using deep wavelet autoencoder-based deep neural network," *IEEE Access*, vol. 7, pp. 46278–46287, 2019.
- [61] C. Han, L. Rundo, R. Araki, Y. Nagano, Y. Furukawa, G. Mauri, H. Nakayama, and H. Hayashi, "Combining noise-to-image and Image-to-Image GANs: Brain MR image augmentation for tumor detection," *IEEE Access*, vol. 7, pp. 156966–156977, 2019.
- [62] M. Li, L. Kuang, S. Xu, and Z. Sha, "Brain tumor detection based on multimodal information fusion and convolutional neural network," *IEEE Access*, vol. 7, pp. 180134–180146, 2019.
- [63] T. Hossain, F. S. Shishir, M. A. Ashraf, M. A. Al Nasim, and F. Muhammad Shah, "Brain tumor detection using convolutional neural network," in *Proc. 1st Int. Conf. Adv. Sci., Eng. Robot. Technol. (ICASERT)*, May 2019, pp. 1–6.
- [64] S. Noman Qasem, A. Nazar, A. Qamar, S. Shamshirband, and A. Karim, "A learning based brain tumor detection system," *Comput., Mater. Continua*, vol. 59, no. 3, pp. 713–727, 2019.

- [65] J. Amin, M. Sharif, M. Raza, T. Saba, R. Sial, and S. A. Shad, "Brain tumor detection: A long short-term memory (LSTM)-based learning model," *Neural Comput. Appl.*, vol. 32, no. 20, pp. 15965–15973, Oct. 2020.
- [66] M. S. Alam, M. M. Rahman, M. A. Hossain, M. K. Islam, K. M. Ahmed, K. T. Ahmed, B. C. Singh, and M. S. Miah, "Automatic human brain tumor detection in MRI image using template-based k means and improved fuzzy c means clustering algorithm," *Big Data Cognit. Comput.*, vol. 3, no. 2, p. 27, May 2019.
- [67] S. Janardhanaprabhu and V. Malathi, "Brain tumor detection using depth-first search tree segmentation," *J. Med. Syst.*, vol. 43, no. 8, pp. 1–12, Aug. 2019.
- [68] P. G. Rajan and C. Sundar, "Brain tumor detection and segmentation by intensity adjustment," *J. Med. Syst.*, vol. 43, no. 8, pp. 1–13, Aug. 2019.
- [69] M. M. Thaha, K. P. M. Kumar, B. Murugan, S. Dhanasekaran, P. Vijayarathinam, and A. S. Selvi, "Brain tumor segmentation using convolutional neural networks in MRI images," *J. Med. Syst.*, vol. 43, no. 9, pp. 1–10, 2019.
- [70] N. Noreen, S. Palaniappan, A. Qayyum, I. Ahmad, M. Imran, and M. Shoaib, "A deep learning model based on concatenation approach for the diagnosis of brain tumor," *IEEE Access*, vol. 8, pp. 55135–55144, 2020.
- [71] M. Sharif, J. Amin, M. Raza, M. A. Anjum, H. Afzal, and S. A. Shad, "Brain tumor detection based on extreme learning," *Neural Comput. Appl.*, vol. 32, no. 20, pp. 15975–15987, Oct. 2020.
- [72] P. Saxena, A. Maheshwari, and S. Maheshwari, "Predictive modeling of brain tumor: A deep learning approach," in *Advances in Intelligent Systems and Computing*. Cham, Switzerland: Springer, 2021, pp. 275–285.
- [73] E. M. Senan, M. E. Jadhav, T. H. Rassem, A. S. Aljaloud, B. A. Mohammed, and Z. G. Al-Mekhlafi, "Early diagnosis of brain tumour MRI images using hybrid techniques between deep and machine learning," *Comput. Math. Methods Med.*, vol. 2022, pp. 1–17, May 2022.
- [74] H. Yahyaoui, F. Ghazouani, and I. R. Farah, "Deep learning guided by an ontology for medical images classification using a multimodal fusion," in *Proc. Int. Congr. Adv. Technol. Eng. (ICOTEN)*, Jul. 2021, pp. 1–6.
- [75] A. R. Khan, S. Khan, M. Harouni, R. Abbasi, S. Iqbal, and Z. Mehmood, "Brain tumor segmentation using K-means clustering and deep learning with synthetic data augmentation for classification," *Microsc. Res. Technique*, vol. 84, no. 7, pp. 1389–1399, Jul. 2021.
- [76] G. Latif, G. Ben Brahim, D. N. F. A. Iskandar, A. Bashar, and J. Alghazo, "Glioma Tumors" classification using deep-neural-network-based features with SVM classifier," *Diagnostics*, vol. 12, no. 4, p. 1018, Apr. 2022.
- [77] A. Pashaie, H. Sajedi, and N. Jazayeri, "Brain tumor classification via convolutional neural network and extreme learning machines," in *Proc. 8th Int. Conf. Comput. Knowl. Eng. (ICCKE)*, Oct. 2018, pp. 314–319.
- [78] A. Gumaei, M. M. Hassan, M. R. Hassan, A. Alelaiwi, and G. Fortino, "A hybrid feature extraction method with regularized extreme learning machine for brain tumor classification," *IEEE Access*, vol. 7, pp. 36266–36273, 2019.
- [79] Z. N. K. Swati, Q. Zhao, M. Kabir, F. Ali, Z. Ali, S. Ahmed, and J. Lu, "Brain tumor classification for MR images using transfer learning and fine-tuning," *Computerized Med. Imag. Graph.*, vol. 75, pp. 34–46, Jul. 2019.
- [80] S. Patil and D. Kirange, "Ensemble of deep learning models for brain tumor detection," *Proc. Comput. Sci.*, vol. 218, pp. 2468–2479, Jan. 2023.

SAMAR M. ALQHTANI received the Ph.D. degree in information technology from The University of Newcastle, Australia. She is currently an Associate Professor with Najran University, Saudi Arabia. She has lectured and developed curricula for courses in computer science and information systems and worked to develop quality in the university sector. Recently, she has led and worked on various projects, including event detection applications in social media, medical applications, and applying artificial intelligence and machine learning algorithms to emerging technologies. Her research interests include information technology and multimedia, including artificial intelligence, machine learning, deep learning, health informatics, data mining, image processing, computer vision, text processing, information security, and internet-oriented IT applications.



TOUFIQUE AHMED SOOMRO (Senior Member, IEEE) received the Ph.D. degree in AI and image processing from Charles Sturt University, Australia, in 2018. He is currently an Associate Professor and the Head with the Department of Electronic Engineering, The University of Larkano, Pakistan. He is an accomplished academic with expertise in engineering and artificial intelligence (AI). He has made significant contributions to the field, with 61 research publications in AI for medical imaging. He has collaborated on projects related to AI for biomedical imaging with the Ministry of Education, Saudi Arabia, and Najran University. In addition, he was honored as a Young Research Professor with Guangdong University of Technology, China, from 2019 to 2020. With his extensive knowledge and research expertise, he continues to advance the field of AI and image processing. As an Educator, he inspires students and contributes to the growth of electronic engineering. His accomplishments demonstrate his commitment to research excellence and his contributions to the scientific community. His research interests include image enhancement, segmentation, classification, and analysis for medical images.



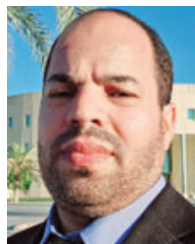
AHMED ALI SHAH (Senior Member, IEEE) received the B.E. degree in electronic engineering from Mehran University of Engineering and Technology, Jamshoro, in 2010. In 2012, he received the prestigious Higher Education Commission (HEC) Pakistan fully-funded HRDI-UET/USTPs Scheme Scholarship, for the M.S. studies leading to the Ph.D. studies from Hanyang University's Education Research Industry Cluster Ansan (E.R.I.C.A.) Campus, South Korea. He has around eight years of diverse experience in academia, industry, and research. Over the past few years, he has participated in several industrial projects and received various technical training and certifications. He has hands-on experience in the soft fabrication of photonic-based sensing and imaging nanoplatforms, specifically his focus was to improve the limit of detection values (LODs), which in turn enhances sensitivity and minimizes safety risks. His research interests include surface-enhanced Raman scattering (SERS)-based sensing and imaging, anisotropic electric field responsive nanostructures, and smart sensors. To date, his research work has been disseminated to international audiences, in the form of patents, book chapters, SCI research journal articles, and peer-reviewed international conference proceedings.



ABDUL AZIZ MEMON (Member, IEEE) received the B.Eng. degree in telecommunication engineering from the Mehran University of Engineering and Technology, Pakistan, in 2007, and the M.S. and Ph.D. degrees from the Department of Electronic and Computer Engineering, Hanyang University, South Korea, in 2010 and 2018, respectively. Soon after completing the B.Eng. degree, he served for more than a year with Huawei Technologies Company Ltd. as a Management Service Engineer for DWDM optical networks for cellular companies. Since January 2012, he has been with Sukkur IBA University, where he is currently an Associate Professor with the Department of Electrical Engineering. Before joining Sukkur IBA University, he was an Assistant Professor with the Department of Electrical Engineering, Isra University, Pakistan. He has more than 15 years of experience in academia and industry. His research interests include protocol design and testing for wireless sensor networks, wireless mobile communication, and delay-tolerant networks. He received a fully-funded scholarship from the HEC Government of Pakistan for the M.S. and Ph.D. studies.



MUHAMMAD IRFAN received the Ph.D. degree in electrical and electronic engineering from Universiti Teknologi PETRONAS, Malaysia, in 2016. He has two years of industry experience (October 2009–October 2011) and six years of academic experience (since January 2017) in teaching and research. He is currently an Associate Professor with the Electrical Engineering Department, Najran University, Saudi Arabia. He has authored more than 200 research papers in reputed journals, books, and conference proceedings (Google Scholar Citations of 2400 and H-index of 22). His research interests include automation and process control, energy efficiency, condition monitoring, vibration analysis, artificial intelligence, the Internet of Things (IoT), big data analytics, smart cities, and smart healthcare.



ABDULKAREM H. M. ALMAWGANI received the B.Sc. degree in information engineering from the College of Engineering, Baghdad University, in 2003, and the M.Sc. degree in electronic systems design engineering and the Ph.D. degree in communication engineering from Universiti Sains Malaysia, in 2008 and 2011, respectively. He was an Assistant Professor with the Department of Electrical Engineering, Faculty of Engineering, University of Science and Technology, Sana'a, Yemen, until February 2014, when he moved to Najran University, Saudi Arabia, where he was promoted to an Associate Professor with the Electrical Engineering Department, College of Engineering. His main research interests include signal-processing algorithms with applications to telecommunications and wireless communication networks.



smart cities, and smart healthcare.

SAIFUR RAHMAN received the Ph.D. degree in electrical and electronics engineering. He has more than 12 years of academic experience in teaching and research. He is currently an Associate Professor with the College of Engineering, Najran University, Saudi Arabia. He has authored more than 70 research articles in reputed journals, books, and conference proceedings. His main research interests include artificial intelligence, the Internet of Things (IoT), big data analytics, smart cities, and smart healthcare.



His research interests include the synthesis and characterization of nanomaterials and quantum dots and the fabrication of devices for energy, sensors, and photocatalysis applications.

MOHAMMED JALALAH received the B.Sc. degree from the King Fahd University of Petroleum and Minerals (KFUPM), in 2001, the M.Sc. degree from The University of Manchester, U.K., in 2009, and the Ph.D. degree from Hanyang University, Republic of Korea, in 2018. He is currently an Associate Professor with the Department of Electrical Engineering and the Promising Centre for Sensors and Electronic Devices (PCSED), Najran University, Saudi Arabia.

LADON AHMED BADE ELJAK received the B.Sc. and master's degrees (Hons.) in electronics engineering from Sudan University of Science and Technology (SUST), Khartoum, Sudan, in 2005 and 2010, respectively, and the Ph.D. degree in electrical and electronics engineering from Universiti Teknologi PETRONAS, Malaysia, in 2019. She was a Lecturer with Sudan Technological University (STU), the University of Medical Sciences and Technology (UMST), the Mohamed Said Hag Secondary School for Gifted Students, the Al-Manhal University Academy of Sciences, Sudan University of Science and Technology (SUST), and Elnwabeg Private Secondary School for Girls, Khartoum. She was an Engineer with ALFA Trading Enterprises Company Ltd., Khartoum, for one year. She is currently an Assistant Professor with the Department of Electrical and Electronics Engineering, Sudan Technological University. Her main research interests include RF MEMS, tunable combined band-pass filters, MetalMUMPs, digital electronic circuits, electronics measurements, microprocessor-based systems, analog communication, digital communication, microwave engineering, communication systems, antenna communication, fiber optic communication, mobile and satellite communication, power electronics, electronics, measurement and instrumentation, renewable energy and energy systems, machine learning, and data analysis.

...